ANALYSIS OF CAPSULE R FROM THE WISCONSIN ELECTRIC POWER COMPANY POINT BEACH NUCLEAR PLANT UNIT NO. 2 REACTOR VESSEL RADIATION SURVEILLANCE PROGRAM (WCAP-9635) EPRI RESEARCH PROJECT 1021-3 TOPICAL REPORT

December 1979

Prepared by

WESTINGHOUSE ELECTRIC CORPORATION
Nuclear Technology Division
P. O. Box 355
Pittsburgh, Pennsylvania 15230

T. R. Mager, Principal Investigator

Prepared for

ELECTRIC POWER RESEARCH INSTITUTE
3412 Hillview Avenue
Palo Alto, California 94304

Project Manager
T. U. Marston

ANALYSIS OF CAPSULE R FROM THE WISCONSIN ELECTRIC POWER COMPANY POINT BEACH NUCLEAR PLANT UNIT NO. 2 REACTOR VESSEL RADIATION SURVEILLANCE PROGRAM (WCAP-9635) EPRI RESEARCH PROJECT 1021-3 TOPICAL REPORT

S. E. Yanichko
S. L. Anderson
R. P. Shogan
R. G. Lott

December 1979

Prepared by

WESTINGHOUSE ELECTRIC CORPORATION
Nuclear Technology Division
P. O. Box 355
Pittsburgh, Pennsylvania 15230

T. R. Mager, Principal Investigator

Prepared for

ELECTRIC POWER RESEARCH INSTITUTE
3412 Hillview Avenue
Palo Alto, California 94304

Project Manager
T. U. Marston

LEGAL NOTICE

This report was prepared by Westinghouse Electric Corporation (WESTINGHOUSE) as an account of work sponsored by the Electric Power Research Institute, Inc. (EPRI). Neither EPRI, members of EPRI, nor WESTINGHOUSE, nor any person acting on behalf of either:

a. Makes any warranty or representation, express or implied, with respect to the accuracy, completeness, or usefulness of the information contained in this report, or that the use of any information, apparatus, method, or process disclosed in this report may not infringe privately owned rights; or

b. Assumes any liabilities with respect to the use of, or for damages resulting from the use of, any information, apparatus, method, or process disclosed in this report.

TABLE OF CONTENTS

LIST OF ILLUSTRATIONS

LIST OF ILLUSTRATIONS (cont)

LIST OF TABLES

LIST OF TABLES (cont)

SECTION 1
SUMMARY OF RESULTS

The analysis which compared unirradiated with irradiated material properties of the reactor vessel material contained in the third surveillance capsule, designated Capsule R from the Wisconsin Electric Power Company Point Beach Nuclear Plant Unit No. 2 reactor pressure vessel, led to the following conclusions.

The capsule received an average fast fluence of $2.01 \times 10^{19} n/cm^2$ ($E > 1$ mev).

The predicted fast fluence for the capsule was $2.14 \times 10^{19} n/cm^2$ ($E > 1$ mev).

The fast fluence of $2.01 \times 10^{19} n/cm^2$ resulted in a 128°C (230°F) increase in the 41 joule (30 ft lb) transition temperature of the weld metal which is the most limiting material in the core region of the reactor vessel. No increase in the 68 joule (50 ft lb) transition temperature was determined for the weld metal since the average shelf energy of the material was only 63.5 joule (47 ft lb). The weld heat-affected-zone material exhibited a 68 joule transition temperature increase of 108°C (195°F).

The intermediate shell forging 123V500VA1 and lower shell forging 122W195VA1 exhibited a 68 joule transition temperature increase of 39°C (70°F) and 17°C (30°F) respectively after irradiation to $2.01 \times 10^{19} n/cm^2$.

ASTM A533 Grade B Class 1 reference correlation monitor material (HSST Plate 02) showed an increase of 88°C (159°F) in the 68 joule transition temperature after irradiating to $2.01 \times 10^{19} n/cm^2$.

A comparison of test results from Capsule R with earlier capsules irradiated to 6.53 and $8.29 \times 10^{18} n/cm^2$ indicates that irradiation to $2.01 \times 10^{19} n/cm^2$ did not result in radiation damage saturation as observed for Point Beach Unit No. 1 surveillance material.

End-of-life projected fast neutron fluences for the reactor vessel, based on 32 full-power years of operation at 1518 Mw, are as follows:

Vessel Location	Fast Neutron Fluence (n/cm^2) Calculated	Measured
Inner surface	3.96×10^{19}	3.90×10^{19}
1/4 thickness	2.64×10^{19}	2.60×10^{19}
3/4 thickness	7.78×10^{18}	7.66×10^{18}

The calculated vessel inner wall fluence after 5.1 EFPY of operation is $6.36 \times 10^{18} n/cm^2$ versus 5.96×10^{18} as determined from surveillance capsule fluence measurements. The difference of approximately 6 percent in the calculated versus measured fast neutron fluence is due in part to the ± 10 percent uncertainty in the measured activities of the fast neutron iron monitors. On the whole, the agreement between calculated and measurement values is considered good.

SECTION 2
INTRODUCTION

This report presents the results of the examination of Capsule R, the third capsule of the continuing surveillance program which monitors the effects of neutron irradiation on the Wisconsin Electric Power Company Point Beach Nuclear Plant Unit No. 2 reactor pressure vessel materials under actual operating conditions.

The surveillance program for the Point Beach Unit No. 2 reactor pressure vessel materials was designed and recommended by the Westinghouse Electric Corporation. Descriptions of the surveillance program and the preirradiation mechanical properties of the reactor vessel materials are presented in WCAP-7712.[1] The surveillance program, planned to cover the 40-year life of the reactor pressure vessel, was based on ASTM E-185-66, "Recommended Practice for Surveillance Tests on Structural Materials in Nuclear Reactors."[2]

This report summarizes testing and the postirradiation data obtained from the third material surveillance capsule (Capsule R) removed from the Point Beach Unit No. 2 reactor vessel, and discusses the analysis of these data. The data are also compared to results of the previously removed Point Beach Unit No. 2 surveillance Capsule V, reported by Battelle Memorial Institute in 1975[3] and Capsule T reported by Westinghouse.[4]

SECTION 3
BACKGROUND

The ability of the large steel pressure vessel containing the reactor core and primary coolant to resist fracture constitutes an important factor in ensuring safety in the nuclear industry. The beltline region of the reactor pressure vessel is the most critical region of the vessel because it is subjected to significant fast neutron bombardment. The overall effects of fast neutron irradiation on the mechanical properties of low-alloy ferritic pressure vessel steels such as SA508 Class 2 (base material of the Unit No. 2 reactor pressure vessel beltline) are well documented in the literature. Generally, low-alloy ferritic materials show an increase in hardness and tensile properties and a decrease in ductility and toughness under certain conditions of irradiation.

A method for performing analyses to guard against fast fracture in reactor pressure vessels is presented in "Protection Against Non-ductile Failure," Appendix G to Section III of the ASME Boiler and Pressure Vessel Code. The method utilizes fracture mechanics concepts and is based on the reference nil-ductility temperature, RT_{NDT}.

RT_{NDT} is defined as the greater of the drop weight nil-ductility transition temperature (NDTT per ASTM E-208) or the temperature 60°F less than the 50 ft-lb temperature (or 35 mil lateral expansion temperature if this is greater) as determined from Charpy specimens oriented normal to the rolling direction of the material. The RT_{NDT} of a given material is used to index that material to a reference stress-intensity factor curve (K_{IR} curve) which appears in Appendix G of the ASME Code. The K_{IR} curve is a lower bound of dynamic, crack arrest, and static fracture toughness results obtained from several heats of pressure vessel steel. When a given material is indexed to the K_{IR} curve, allowable stress-intensity factors can be obtained for this material as a function of temperature. Allowable operating limits can then be determined utilizing these allowable stress-intensity factors.

RT_{NDT}, and in turn the operating limits of nuclear power plants, can be adjusted to account for the effects of radiation on the reactor vessel material properties. The radiation embrittlement or changes in mechanical properties of a given reactor pressure vessel steel can be monitored by a reactor surveillance program such as the Point Beach Nuclear Plant Unit No. 2

Reactor Vessel Radiation Surveillance Program,[1] in which a surveillance capsule is periodically removed from the operating nuclear reactor and the encapsulated specimens are tested. The increase in the Charpy V-notch temperature (ΔRT_{NDT}) due to irradiation is added to the original RT_{NDT} to adjust the RT_{NDT} for radiation embrittlement. This adjusted RT_{NDT} (RT_{NDT} initial + ΔRT_{NDT}) is used to index the material to the K_{IR} curve and in turn to set operation limits for the nuclear power plant which take into account the effect of irradiation on the reactor vessel materials.

SECTION 4
DESCRIPTION OF PROGRAM

Six surveillance capsules for monitoring the effects of neutron exposure on the Point Beach Nuclear Plant Unit No. 2 reactor pressure vessel core region material were inserted in the reactor vessel prior to initial plant startup. The six capsules were positioned in the reactor vessel between the thermal shield and the vessel wall at locations shown in figure 4-1. The vertical center of the capsules is opposite the vertical center of the core.

Capsule R was removed after approximately 6.5 calendar years (5.1 effective full-power years) of plant operation. This capsule contained Charpy V-notch impact, tensile, and WOL specimens (shown in WCAP-7712) from the intermediate and lower ring forgings, weld metal representative of the core region of the reactor vessel, and Charpy V-notch specimens from weld-heat-affected-zone (HAZ) material. The capsule also contained Charpy V-notch specimens from the 12-inch-thick ASTM A533 Grade B Class 1 correlation monitor material furnished by Oak Ridge National Laboratory from HSST Plate 02. The chemistry and heat treatment of the surveillance material are presented in tables 4-1 and 4-2.

All test specimens were machined from the 1/4-thickness location of the forgings. Test specimens represent material taken at least one forging thickness from the quenched end of the forging. All base metal Charpy V-notch and tensile specimens were oriented with the longitudinal axis of the specimen parallel to the principal working direction of the forgings. The WOL test specimens were machined with the crack plane of the specimen perpendicular to the surfaces and working direction of the forgings.

Charpy V-notch specimens from the weld metal were oriented with the longitudinal axis of the specimens transverse to the weld direction. Tensile specimens were oriented with the longitudinal axis of the specimen parallel to the weld.

Capsule R contained dosimeter wires of copper, nickel, and aluminum-0.15 wt. percent cobalt (cadmium-shielded and unshielded). In addition, the capsule contained cadmium-shielded dosimeters of Np-237 and U-238, located as shown in figure 4-2.

TABLE 4-1

CHEMISTRY AND HEAT TREATMENT OF MATERIAL REPRESENTING THE CORE REGION SHELL FORGINGS AND WELD METAL FROM THE POINT BEACH UNIT NO. 2 REACTOR VESSEL

	Chemical Analyses (percent)		
Element	Forging 123V500VA1	Forging 122W195VA1	Weld Metal
C	0.20	0.22	0.079
Mn	0.65	0.59	1.40
P	0.009	0.010	0.014
S	0.009	0.008	0.013
Si	0.24	0.23	0.55
Mo	0.59	0.60	0.39
Cu	0.088	0.051	0.25
Ni	0.71	0.70	0.59
Cr	0.35	0.33	0.07
Al	<0.005	<0.005	<0.005
N_2	0.004	0.002	0.010
V	0.010	0.010	<0.002
Co	0.004	0.010	0.013

Heat Treatment

Forging 123V500VA1	Heated at 1550°F, 9½ hours, water-quenched Tempered at 1200°F, 12 hours, air-cooled Stress-relieved at 1125°F, 12 hours, furnace-cooled
Forging 122W195VA1	Heated at 1550°F, 8 hours, water-quenched Tempered at 1200°F, 12 hours, air-cooled Stress-relieved at 1125°F, 12 hours, furnace-cooled
Weldment	Stress-relieved at 1125°F, 11½ hours, furnace-cooled

TABLE 4-2

CHEMISTRY AND HEAT TREATMENT OF SURVEILLANCE MATERIAL REPRESENTING 12-INCH-THICK A533 GRADE B CLASS 1 CORRELATION MONITOR MATERIAL (HSST Plate 02)

Chemical Analysis								
	C	Mn	P	S	Si	Ni	Mo	Cu
Ladle	0.22	1.45	0.011	0.019	0.22	0.62	0.53	---
Check	0.22	1.48	0.012	0.018	0.25	0.68	0.52	0.14

Heat Treatment

1675 ± 25°F – 4 hours – Air-cooled
1600 ± 25°F – 4 hours – Water-quenched
1125 ± 25°F – 4 hours – Furnace-cooled
1150 ± 25°F – 40 hours – Furnace-cooled to 600°F

Thermal monitors made from two low-melting eutectic alloys and sealed in Pyrex tubes were included in the capsule and were located as shown in figure 4-2. The two eutectic alloys and their melting points are:

2.5% Ag, 97.0% Pb	Melting Point 304°C (579°F)
1.75% Ag, 0.75% Sn, 97.5% Pb	Melting Point 310°C (590°F)

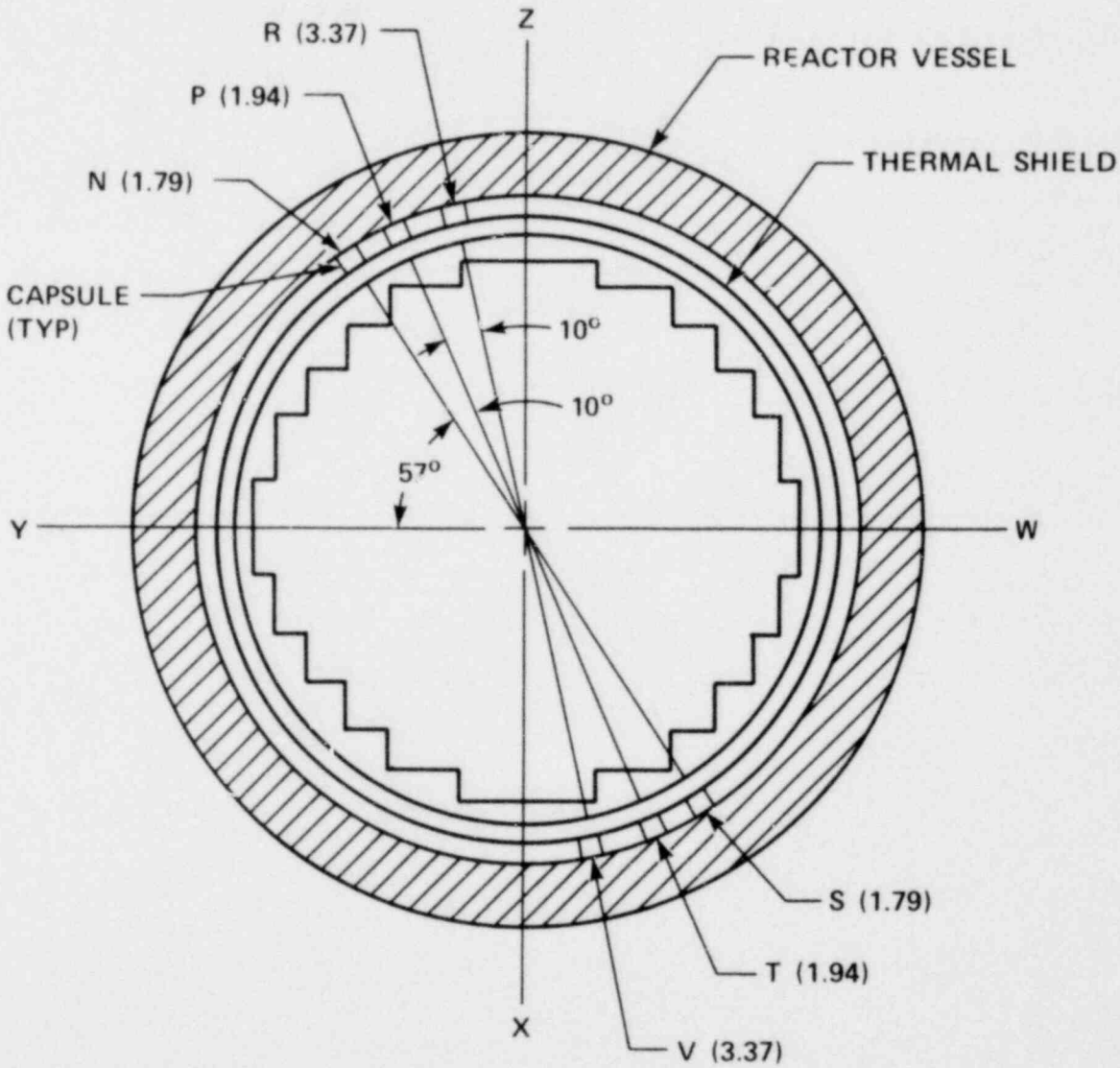

Figure 4-1. Arrangement of Surveillance Capsules in the Point Beach Unit No. 2 Reactor Vessel (Lead Factors for the Capsules are Shown in Parentheses)

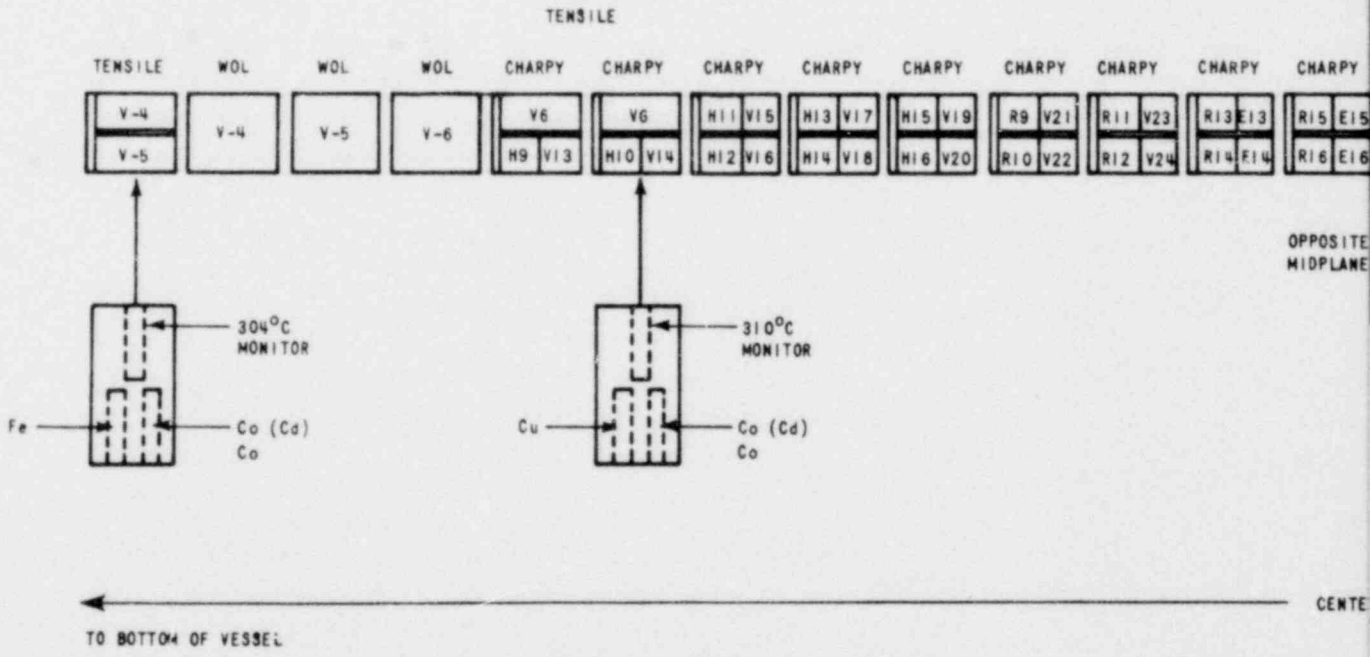
TENSILE
TENSILE
WOL
WOL
WOL
CHARPY
CHARPY
CHARPY
CHARPY
CHARPY
CHARPY
CHARPY
CHARPY
V-4
V-5
V-4
V-5
V-6
V6
H9
V13
V6
H10
V14
H11
V15
H12
V16
H13
V17
H14
V18
H15
V19
H16
V20
R9
V21
R10
V22
R11
V23
R12
V24
R13
E13
R14
E14
R15
E15
R16
E16
OPPOSITE
MIDPLANE
304°C
MONITOR
Fe
Co (Cd)
Co
310°C
MONITOR
Cu
Co (Cd)
Co
CENTE
TO BOTTOM OF VESSEL

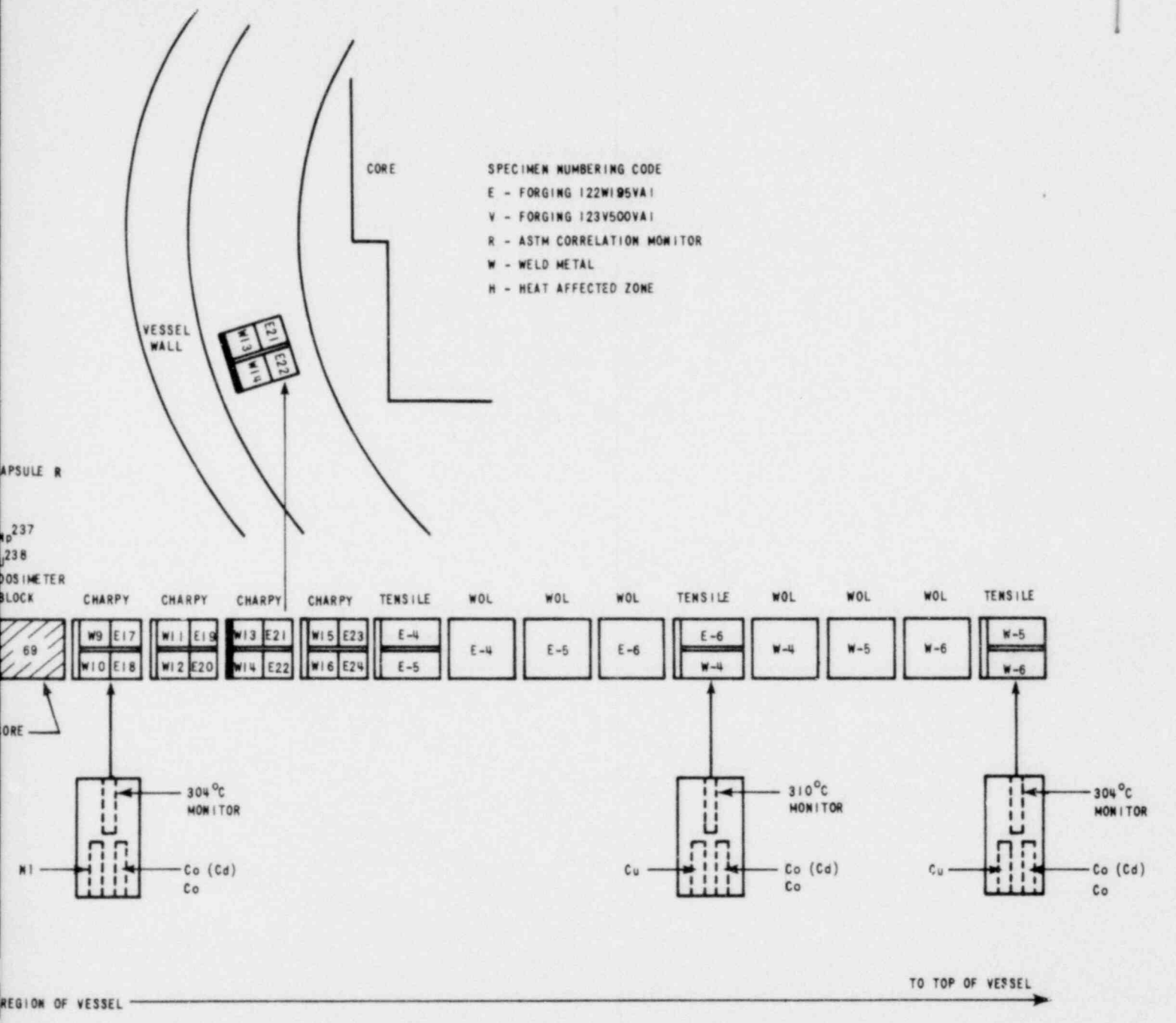

Figure 4-2. Capsule R Schematic Diagram Showing Designed Arrangement of Specimens, Thermal Monitors, and Dosimeter Placement and Orientation with Respect to the Core and Vessel Wall

SECTION 5
TESTING OF SPECIMENS FROM CAPSULE R

The postirradiation mechanical testing of the Charpy V-notch and tensile specimens was performed at the Westinghouse Research and Development Laboratory with consultation by Westinghouse Nuclear Energy Systems personnel. Testing was performed in accordance with 10CFR50, Appendices G and H.

Upon receipt of the capsule at the laboratory, the specimens and spacer blocks were carefully removed, inspected for identification number, and checked against the master list in WCAP-7712.[1] No discrepancies were found.

Examination of the two low-melting 304°C (579°F) and 310°C (590°F) eutectic alloys indicated no melting of either type of thermal monitor. Based on this examination, the maximum temperature to which the test specimens were exposed was less than 304°C (579°F).

The Charpy impact tests were performed on a Tinius-Olsen Model 74, 358J machine. The tup (striker) of the Charpy machine is instrumented with an Effects Technology model 500 instrumentation system. With this system, load-time and energy-time signals can be recorded in addition to the standard measurement of Charpy energy (E_D). From the load-time curve, the load of general yielding (P_{GY}), the time to general yielding (t_{GY}), the maximum load (P_M), and the time to maximum load (t_M) can be determined. Under some test conditions, a sharp drop in load indicative of fast fracture was observed. The load at which fast fracture was initiated is identified as the fast fracture load (P_F), and the load at which fast fracture terminated is identified as the arrest load (P_A).

The energy at maximum load (E_M) was determined by comparing the energy-time record and the load-time record. The energy at maximum load is roughly equivalent to the energy required to initiate a crack in the specimen. Therefore, the propagation energy for the crack (Ep) is the difference between the total energy to fracture (E_D) and the energy at maximum load.

The yield stress (σ_y) is calculated from the three point bend formula. The flow stress is calculated from the average of the yield and maximum loads, also using the three point bend formula.

Percent shear was determined from postfracture photographs using the ratio-of-areas method in compliance with ASTM Specification A370-74. The lateral expansion was measured using a dial gage rig similar to that shown in the same specification.

Tensile tests were performed on a 20,000 lb Instron, split-console test machine (Model 1115) per ASTM Specifications E8 and E21, and MHL Procedure 7604 Revision 2. All pull rods, grips and pins were made of Inconel 718 hardened to R_c 45. The upper pull rod was connected through a universal joint to improve axiality of loading.

The tests were conducted at a constant crosshead speed of 0.05 inches/minute throughout the test.

Deflection measurements were made with a linear variable displacement transducer (LVDT) extensometer. The extensometer knife edges were spring-loaded to the specimen and operated through specimen failure. The extensometer gage length is 1.00 inches. The extensometer is rated as Class B-2 per ASTM E83.

Elevated test temperatures were obtained with a three-zone electric resistance split-tube furnace with a 9-inch hot zone. All tests were conducted in air.

Because of the difficulty in remotely attaching a thermocouple directly to the specimen, the following procedure was used to monitor specimen temperature:

> Chromel-alumel thermocouples were inserted in shallow holes in the center and each end of the gage section of a dummy specimen and in each grip. In test configuration, with a slight load on the specimen, a plot of specimen temperature versus upper and lower grip and controller temperatures was developed over the range room temperature to 550°F. The upper grip was used to control the furnace temperature.
>
> During the actual testing the grip temperatures were used to obtain desired specimen temperatures. Experiments indicated that this method is accurate to ± 2°F.

The yield load, ultimate load, fracture load, total elongation, and uniform elongation were determined directly from the load-extension curve. The yield strength, ultimate strength, and fracture strength were calculated using the original cross-sectional area. The final diameter and final gage length were determined from postfracture photographs. The fracture area used to calculate the fracture stress (true stress at fracture) and percent reduction in area was computed using the final diameter measurement.

5-1. CHARPY V-NOTCH IMPACT TEST RESULTS

The results of tests performed on the various materials in Capsule R are presented in tables 5-1 through 5-6 and figures 5-1 through 5-5. The results of tests performed on intermediate shell forging 123V500VA1 presented in figure 5-1 and table 5-6 show that irradiation to 2.01 x 10^{19}n/cm^2 increases the 68-joule (50 ft lb) and 41-joule (30 ft lb) temperatures by 39°C (70°F) and increases the 0.9 mm (35 mil) lateral expansion temperature by 47°C (85°F). No decrease in upper shelf energy resulted from irradiation.

The results of tests performed on material from the lower shell forging 122W195VA1 presented in figure 5-2 and table 5-6 show an increase in the 68-joule and 41-joule temperature of 17°C (30°F) and 19°C (35°F), respectively, after irradiation to 2.01 x 10^{19}n/cm^2. The 0.9 mm lateral expansion temperature of this material increased by 29°C (52°F) and the upper shelf energy decreased by 6.5 joules (5 ft lb).

A comparison of the surveillance program test results to date on material from the two core region forgings irradiated to three different neutron fluence levels (6.53, 8.29 and 20.1 x 10^{18}n/cm^2) is presented in table 5-7. The results indicate that both materials are not very sensitive to irradiation, as expected, because of the low copper content levels (< 0.10% Cu) of the forgings. The data indicate that some additional increase in transition temperature did result from irradiation to a fluence of 2.01 x 10^{19}n/cm^2.

Test results obtained on the weld metal presented in figure 5-3 and table 5-6 show that irradiation to 2.01 x 10^{19}n/cm^2 resulted in a 41-joule transition temperature increase of 128°C (230°F). No increase in the 68-joule transition temperature could be determined since the upper shelf energy after irradiation decreased to 63.5 joules. The transition temperature increase measured at the 0.9 mm lateral expansion level was 128°C (230°F) which is identical to the 41-joule transition temperature increase. A comparison of these results for the weld metal versus earlier surveillance capsule results from irradiations to 6.53 and 8.29 x 10^{18}n/cm^2 is shown in table 5-7. This table shows that irradiation to 2.01 x 10^{19}n/cm^2 resulted in a significant additional transition temperature increase rather than a saturation of damage which was inferred from the results of the lower fluence data.

The test results for the weld HAZ material are shown in figure 5-4 and table 5-6. Large scatter is shown in the test results, which appear to follow properties characteristic of either the base or weld material as reflected in the extremely high and low energy values in the upper shelf region. The 68- and 41-joule transition temperature increases for the HAZ material were 108°C (195°F) and 105°C (190°F) respectively. A 92°C (166°F) increase resulted at the 0.9 mm lateral expansion level. The upper shelf energy of the HAZ material after irradiation is higher than the unirradiated shelf. A comparison of the surveillance

IRRADIATED

Sample Number	Test Temp (°C)	Charpy Energy (J)	Lateral Expansion (mm)	Shear (%)	No Charpy Ed/A (KJ/M^2)
V23	-57	5.4	.14	0	67
V14	-32	18.3	.19	0	228
V24	-32	32.5	.60	5	406
V21	-18	52.9	.50	21	660
V20	-18	84.1	1.14	19	1050
V22	-4	72.5	.98	19	906
V17	10	88.1	.98	28	1101
V16	10	145.1	1.77	53	1813
V13	24	200.7	2.11	76	2508
V15	25	280.7	1.75	100	3508
V19	79	235.9	2.07	100	2948
V18	121	252.2	2.11	100	3152

IRRADIATED

Sample Number	Test Temp (°C)	Charpy Energy (J)	Lateral Expansion (mm)	Shear (%)	No Charpy Ed/A (KJ/M^2)
E20	-57	14.2	.16	0	177
E24	-32	12.2	.09	0	152
E17	-32	54.2	.81	15	677
E18	-18	10.8	.25	5	135
E14	-12	40.0	.48	40	499
E22	-4	113.9	1.51	38	1423
E23	-4	80.0	1.02	31	999
E13	24	146.4	1.69	57	1830
E21	49	146.4	1.71	72	1830
E16	79	185.7	1.91	100	2321
E15	96	188.5	1.97	100	2355
E19	121	193.9	1.97	100	2423

TABLE 5-1

ARPY TEST RESULTS FROM SHELL FORGING 123V500VA1

zed Energies									
aximum Em/A$_2$ (KJ/M^2)	Prop Ep/A$_2$ (KJ/M^2)	Yield Load (N)	Time to Yield (Micro Sec)	Maximum Load (N)	Time to Maximum (Micro Sec)	Fracture Load (N)	Arrest Load (N)	Yield Stress (MPa)	Flow Stress (MPa)
59	8	14200	90	14200	90	14200	0		
167	61	16000	100	16900	200	16900	0	824	847
347	59	15600	110	18700	370	18200	0	801	881
491	169	13300	90	18700	500	18700	0	687	824
647	403	14700	95	18700	660	18200	0	755	858
538	368	12000	100	17800	600	17800	0	618	767
631	469	14200	90	18200	660	17300	0	732	835
647	1166	14200	100	18200	660	13800	0	732	835
662	1845	13300	225	17300	725	8000	2700	687	790
768	2739	12500	100	16900	750	0	0	641	755
601	2347	12000	90	16500	760	0	0	618	732
647	2504	12000	100	17300	775	0	0	618	755

TABLE 5-2

ARPY TEST RESULTS FROM SHELL FORGING 122W195VA1

ed Energies									
ximum Em/A$_2$ (KJ/M^2)	Prop Ep/A$_2$ (KJ/M^2)	Yield Load (N)	Time to Yield (Micro Sec)	Maximum Load (N)	Time to Maximum (Micro Sec)	Fracture Load (N)	Arrest Load (N)	Yield Stress (MPa)	Flow Stress (MPa)
167	10	17300	100	18700	210	17800	0	893	927
92	59	16700	135	16900	140	16500	0	858	864
522	155	15600	100	19600	510	19600	0	801	904
67	68	15600	100	16000	130	15600	0	801	812
459	40	15600	100	18700	450	18700	0	801	881
585	838	15600	130	19600	600	16500	0	801	904
506	492	15600	100	19600	510	18700	0	801	904
600	1229	14200	110	18700	600	12900	3600	732	847
662	1167	13800	100	18200	660	13300	5300	709	824
570	1751	13300	125	17300	675	0	0	687	790
570	1785	13300	100	17800	650	0	0	687	801
647	1776	13300	225	16900	725	0	0	687	778

Sample Number	Test Temp (°C)	Charpy Energy (J)	Lateral Expansion (mm)	Shear (%)	Normal Charpy Ed/A (KJ/M^2)
W11	-4	8.8	.20	0	110
W16	24	14.9	.17	0	186
W9	66	25.8	.56	33	322
W12	93	33.9	.52	55	423
W15	121	44.7	.93	90	559
W10	149	67.8	1.07	100	847
W14	177	61.0	.98	100	762
W13	204	62.4	.91	100	779

IRRADIATED CHARPY

Sample Number	Test Temp (°C)	Charpy Energy (J)	Lateral Expansion (mm)	Shear (%)	Normal Charpy Ed/A (KJ/M^2)
H10	-4	23.0	.43	5	288
H9	24	52.9	.62	35	660
H16	52	35.3	.93	48	440
H13	66	146.4	1.71	77	1830
H14	93	65.1	.93	63	813
H11	121	130.2	1.31	98	1626
H15	149	88.1	1.18	100	1101
H12	178	221.0	1.84	100	2762

TABLE 5-3

D CHARPY TEST RESULTS FROM WELD MATERIAL

ed Energies									
ximum Em/A, KJ/M^2)	Prop Ep/A$_2$ (KJ/M^2)	Yield Load (N)	Time to Yield (Micro Sec)	Maximum Load (N)	Time to Maximum (Micro Sec)	Fracture Load (N)	Arrest Load (N)	Yield Stress (MPa)	Flow Stress (MPa)
75	34	16500	100	16500	100	16500	0		
184	2	15600	100	16900	210	16900	0	801	835
233	88	14200	110	16500	280	16500	4400	732	790
266	157	14200	120	16500	300	16000	5300	732	790
315	244	13800	110	16000	360	0	0	709	767
331	516	13300	95	16900	350	0	0	687	778
282	479	13800	105	16000	350	0	0	709	767
282	496	13300	100	16500	340	0	0	687	767

TABLE 5-4

EST RESULTS FROM WELD HEAT-AFFECTED-ZONE MATERIAL

ed Energies									
ximum Em/A, KJ/M^2)	Prop Ep/A$_2$ (KJ/M^2)	Yield Load (N)	Time to Yield (Micro Sec)	Maximum Load (N)	Time to Maximum (Micro Sec)	Fracture Load (N)	Arrest Load (N)	Yield Stress (MPa)	Flow Stress (MPa)
282	5	16500	110	17800	290	17800	0	847	881
522	138	13300	100	19600	530	19600	0	687	847
250	190	14200	100	16900	280	16900	3600	732	801
491	1339	14200	100	18200	500	0	0	732	835
507	306	13800	115	17800	525	16900	8000	709	812
647	979	13800	100	18200	660	0	0	709	824
459	641	13800	100	17300	490	0	0	709	801
723	2038	12500	110	17300	750	0	0	641	767

IRRADIATED
CLASS

Sample Number	Test Temp (°C)	Charpy Energy (J)	Lateral Expansion (mm)	Shear (%)	Normalized Charpy Ed/A (KJ/M^2)	Normalized Maxim Em/ (KJ/M
R14	24	6.1	.04	5	76	4
R12	79	32.5	.67	23	406	29
R13	99	46.1	.70	34	576	42
R11	107	56.9	.99	38	711	49
R10	123	71.9	.76	62	898	37
R9	134	111.2	1.52	52	1389	45
R15	175	130.2	1.68	100	1626	45
R16	204	135.6	2.01	100	1694	49

THE EFFECT OF 288°C
ON THE NO
POINT BEACH

Material	Transition Temperature				
	Unirradiated			Irra	
	50 ft lb 68 Joule °C (°F)	30 ft lb 41 Joule °C (°F)	35 Mil .9 mm °C (°F)	50 ft lb 68 Joule °C (°F)	30 41 °C
123V500VA1	-51 (-60)	-62 (-80)	-59 (-75)	-12 (10)	-2
122W195VA1	-26 (-15)	-42 (-45)	-38 (-37)	-9 (15)	-2
Weld Metal	16 (60)	-18 (0)	-8 (17)	–	11
HAZ Metal (122W195VA1)	-29 (-20)	-62 (-80)	-27 (-16)	79 (175)	43
Correlation Monitor	27 (81)	10 (49)	12 (53)	115 (240)	93

TABLE ' 5

CHARPY TEST RESULTS FROM A533 GRADE B
1 CORRELATION MONITOR MATERIAL

nergies									
m ^{2})	Prop Ep/A $_2$ (KJ/M^2)	Yield Load (N)	Time to Yield (Micro Sec)	Maximum Load (N)	Time to Maximum (Micro Sec)	Fracture Load (N)	Arrest Load (N)	Yield Stress (MPa)	Flow Stress (MPa)
	32	12000	80	12000	80	12000	0		
	107	13800	120	16900	360	16900	5300	709	790
	148	13800	100	17800	460	17800	6700	709	812
	220	13300	100	18200	510	18200	8000	687	812
	518	13300	105	16500	440	0	0	687	767
	930	12900	100	17300	500	0	0	664	778
	1167	10700	60	16900	490	0	0	549	709
	1203	12900	120	17300	520	0	0	664	778

TABLE 5-6

IRRADIATION AT 2.01 x 10^{19} n/cm^2 (E > 1.0 MEV)
TCH TOUGHNESS PROPERTIES OF THE
UNIT NO. 2 REACTOR VESSEL MATERIALS

iated		△ Transition Temperature			Average Energy Absorption at Full Shear				△ Energy	
ft lb Joule (°F)	35 Mil .9 mm °C (°F)	50 ft lb 68 Joule °C (°F)	30 ft lb 41 Joule °C (°F)	35 Mil .9 mm °C (°F)	Unirradiated Joule	ft lb	Irradiated Joule	ft lb	Joule	ft lb
(-10)	-12 (10)	39 (70)	39 (70)	47 (85)	244	180	256	189	+12	+9
(-10)	- 9 (15)	17 (30)	19 (35)	29 (52)	196.5	145	190	140	-6.5	-5
(230)	120 (247)	–	128 (230)	128 (230)	88	65	63.5	47	-24.5	-18
110)	65 (150)	108 (195)	105 (190)	92 (166)	113	83.5	146.5	108	+33.5	+24.5
200)	104 (220)	88 (159)	83 (151)	93 (167)	167.5	123.5	133	98	-34.5	-25.5

TABLE 5-7

SUMMARY OF POINT BEACH UNIT NO. 2
REACTOR VESSEL SURVEILLANCE CAPSULE CHARPY IMPACT TEST RESULTS

Material	Fluence 10^{18} n/cm^2	68 Joule 50 ft lb Trans. Temp Increase (°C)	(°F)	41 Joule 30 ft lb Trans. Temp Increase (°C)	(°F)	Decrease In Upper Shelf Energy (Joule)	(ft lb)
Forging 123V500VA1	6.53	19	35	17	30	None	
" "	8.29	22	40	17	30	None	
" "	20.10	39	70	39	70	None	
Forging 122W195VA1	6.53	8	15	6	10	13.5	10
" "	8.29	7	13	9	17	None	
" "	20.10	17	30	19	35	6.5	5
Weld Metal	6.53	–	–	92	165	31	23
"	8.29	78	140	81	145	12	9
"	20.10	–	–	128	230	24.5	18
HAZ Metal	6.53	–	–	–	–	None	
"	8.29	58	105	61	110	8	6
"	20.10	108	195	105	190	None	
Correlation Monitor	6.53	61	110	50	90	40.5	30
" "	8.29	62	111	58	105	20.5	15
" "	20.10	88	159	83	151	34.5	25.5

program test results to date on the HAZ material is presented in table 5-7. The comparison of data indicates additional transition temperature increase as a result of the 2.01 x 10^{19}n/cm^2 irradiation. Because of the considerable scatter in data for both unirradiated and irradiated tests, the reported transition temperature increases should be considered highly questionable.

Figure 5-5 and table 5-6 present the test results obtained on the A533 Grade B Class 1 ASTM reference correlation monitor material. Irradiation to 2.01 x 10^{19}n/cm^2 resulted in a 68- and 41-joule transition temperature increase of 88°C (159°F) and 83°C (151°F) respectively, and a 0.9 mm lateral expansion increase of 93°C (167°F). Upper shelf energy decreased by 34.5 joules. A comparison of data obtained at three neutron fluence levels from surveillance program capsules is shown in table 5-7. These results show that irradiation to 2.01 x 10^{19}n/cm^2 produced increases in transition temperature greater than those obtained from irradiations at lower fluence levels.

In the summary of results shown in table 5-7, the results of tests from the second surveillance capsule irradiated at the intermediate fluence level indicated that possibly a saturation of radiation damage was occurring. However, a continuation of this saturation was not confirmed by the test results from the third capsule irradiated to 2.01 x 10^{19}n/cm^2. It should be noted that prior to the testing and analysis of the third capsule, including re-evaluation of neutron fluence measurements for earlier capsules, the fluences reported for the first and second capsules were 4.74 and 9.45 x 10^{18}n/cm^2 respectively. Based on these early fluence measurements, the saturation which seemed to be occurring appeared to be real since one would expect significant additional radiation damage at the higher fluence level. However, based on the new revised fluence measurements of 6.53 and 8.29 x 10^{19}n/cm^2, the difference in fluence between the two capsules is not large enough to result in any noticeable difference in radiation damage at the two fluence levels. It is therefore suspected that the saturation of radiation damage observed from tests performed on the second capsule is not a real phenomenon, especially since test results on the third capsule did show additional transition temperature increases. A comparison of the 41-joule transition temperature increases with Westinghouse-predicted 41-joule transition temperature increases is shown in figure 5-6. These results show that none of the 41-joule transition temperature increases exceed the Westinghouse predictions.

Charpy impact specimen fracture surfaces of the various surveillance materials are shown in figures 5-7 through 5-11.

5-2. TENSILE TEST RESULTS

The results of tensile tests performed on the two shell forgings, 123V500VA1 and 122W195VA1, and weld metal at various temperatures from room temperature to 288°C (550°F) are shown in table 5-8. A comparison of the tensile test results for the two forgings after irradiation to three different fluence levels is shown in figures 5-12 and 5-13. The results of the $2.01 \times 10^{19} n/cm^2$ irradiation, when compared with the results of lower irradiation levels, tend to indicate that the tensile properties of the two forgings have saturated. A comparison of the weld metal tensile test results after irradiation to fluence levels of 6.53 and $20.1 \times 10^{18} n/cm^2$ is shown in figure 5-14. This comparison shows that irradiation resulted in significantly high increases in 0.2-percent yield strength, indicating that the material is highly sensitive to irradiation. The irradiation at $2.01 \times 10^{19} n/cm^2$ which resulted in additional increased yield strength over that resulting from irradiation at $6.53 \times 10^{18} n/cm^2$ tends to confirm the additional increase in transition temperature which occurred.

Photographs of the fractured tensile specimens from the two forgings and the weld metal are shown in figures 5-15 through 5-17 respectively. A typical stress-strain curve for the tensile tests is shown in figure 5-18.

5-3. WEDGE OPENING LOADING TESTS

Wedge Opening Loading (WOL) fracture mechanics specimens which were contained in the surveillance capsule have been stored at the Westinghouse Research Laboratory at the request of the Wisconsin Electric Power Company on the recommendation of the U.S. Nuclear Regulatory Commission; they will be tested and reported later.

TABLE 5-8

TENSILE PROPERTIES FOR POINT BEACH UNIT NO. 2 PRESSURE VESSEL MATERIAL IRRADIATED TO 2.01×10^{19} n/cm^2

Sample Number	Test Temperature (°C)	Yield Strength (MPa)	Ultimate Strength (MPa)	Fracture Load (N)	Fracture Stress (MPa)	Fracture Strength (MPa)	Ultimate Elongation (%)	Total Elongation (%)	Reduction in Area (%)
E-4	27	541	653	13,300	1270	419	8.7	22.5	67
E-5	149	503	618	13,000	1290	412	8.4	20.6	68
E-6	288	470	625	13,500	1380	427	8.7	20.6	69
V-4	27	441	597	11,900	1340	375	10.7	25.2	72
V-5	149	401	548	11,200	1260	354	9.5	22.8	72
V-6	288	387	554	11,900	1390	375	10.2	22.5	73
W-4	27	657	738	17,600	1390	555	9.8	20.9	60
W-5	149	597	684	17,000	1110	535	8.7	18.8	52
W-6	288	573	688	17,600	1210	555	8.2	16.7	54

Samples E-4, E-5, and E-6 are 122W195VA1 material

Samples V-4, V-5, and V-6 are 123V500VA1 material

Samples W-4, W-5, and W-6 are weld metal

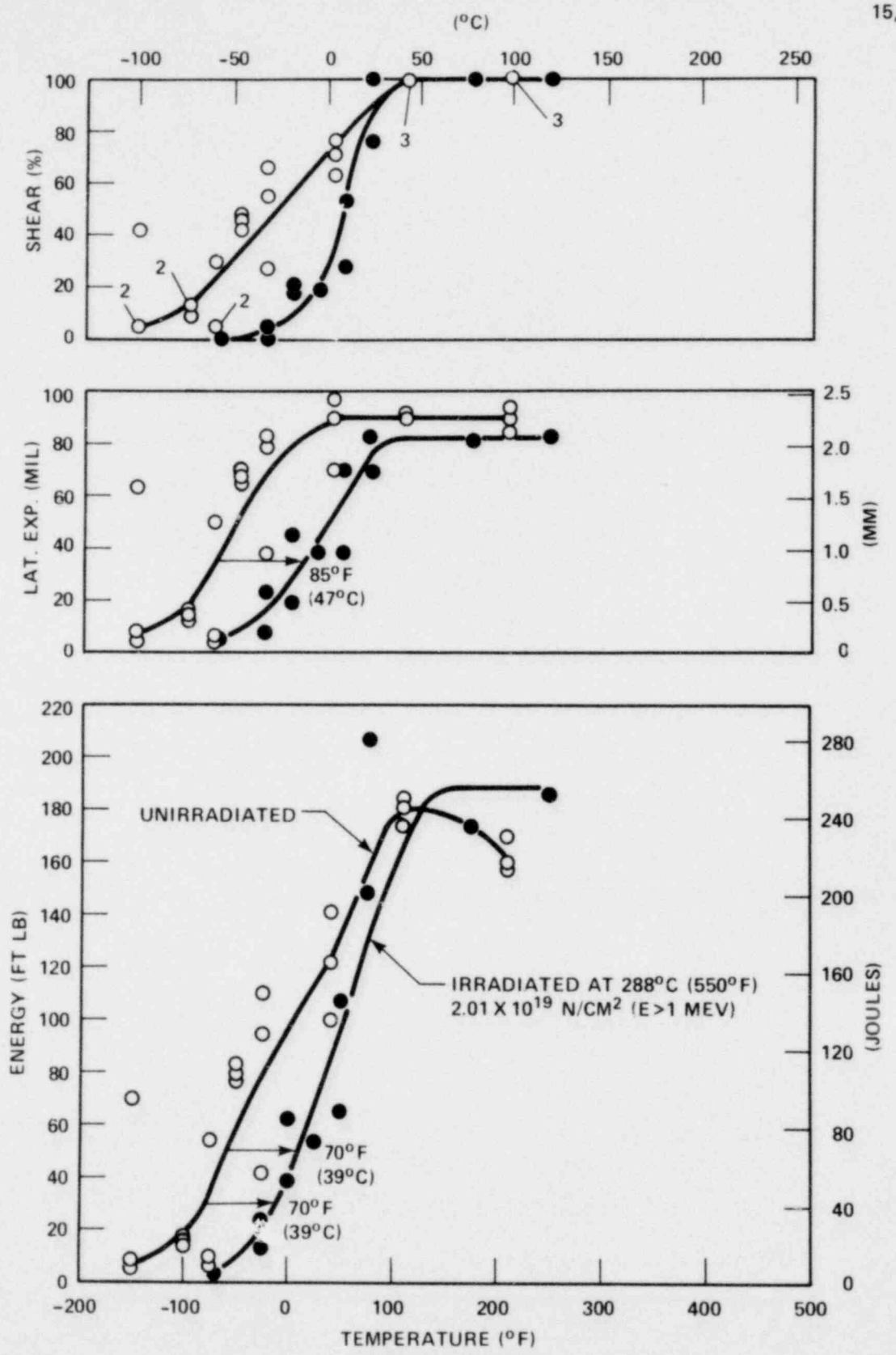

Figure 5-1. Charpy V-Notch Impact Data for the Point Beach Unit No. 2 Pressure Vessel Intermediate Shell Forging 123V500VA1

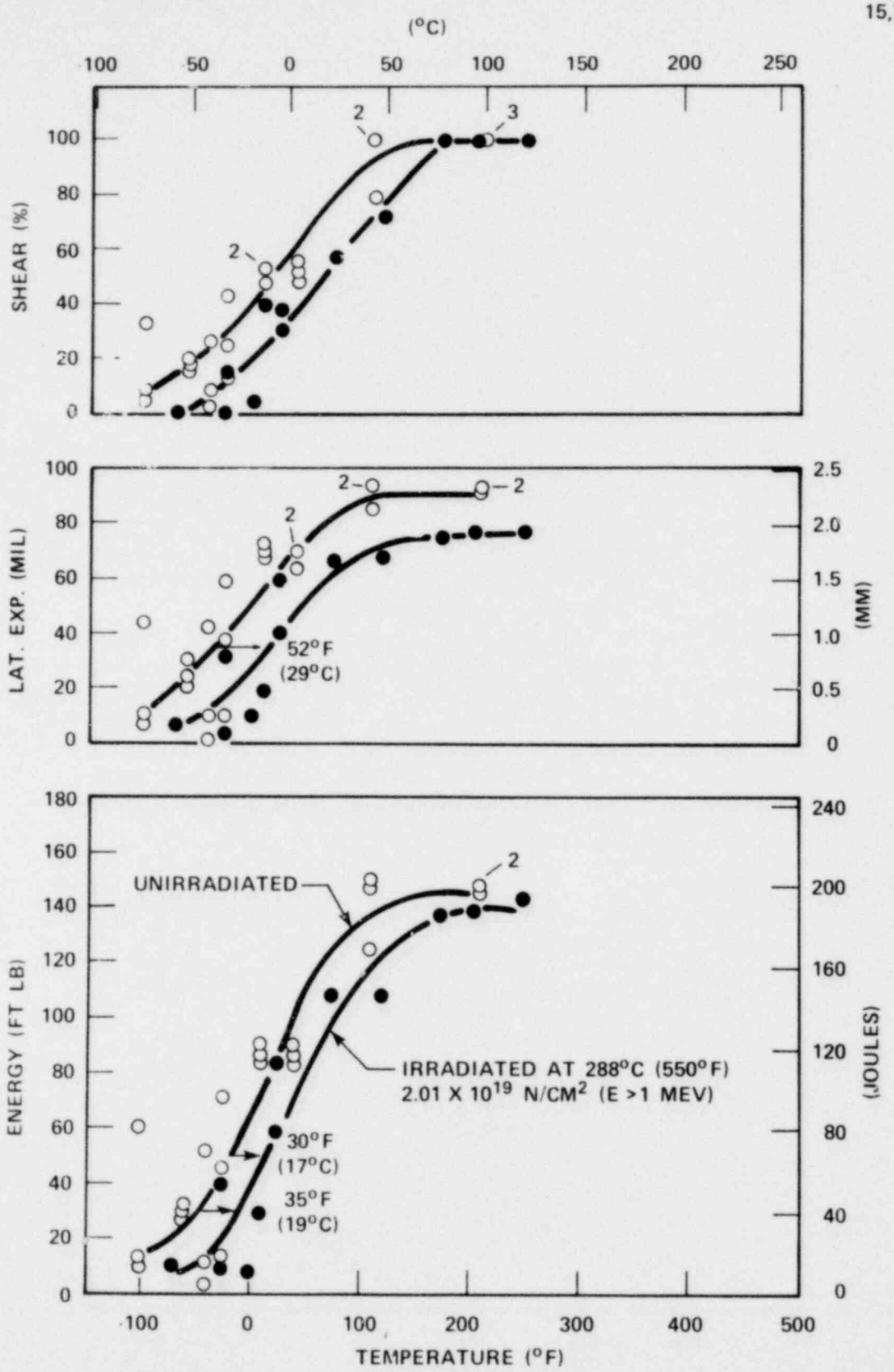

Figure 5-2. Charpy V-Notch Impact Data for the Point Beach Unit No. 2 Pressure Vessel Lower Shell Forging 122W195VA1

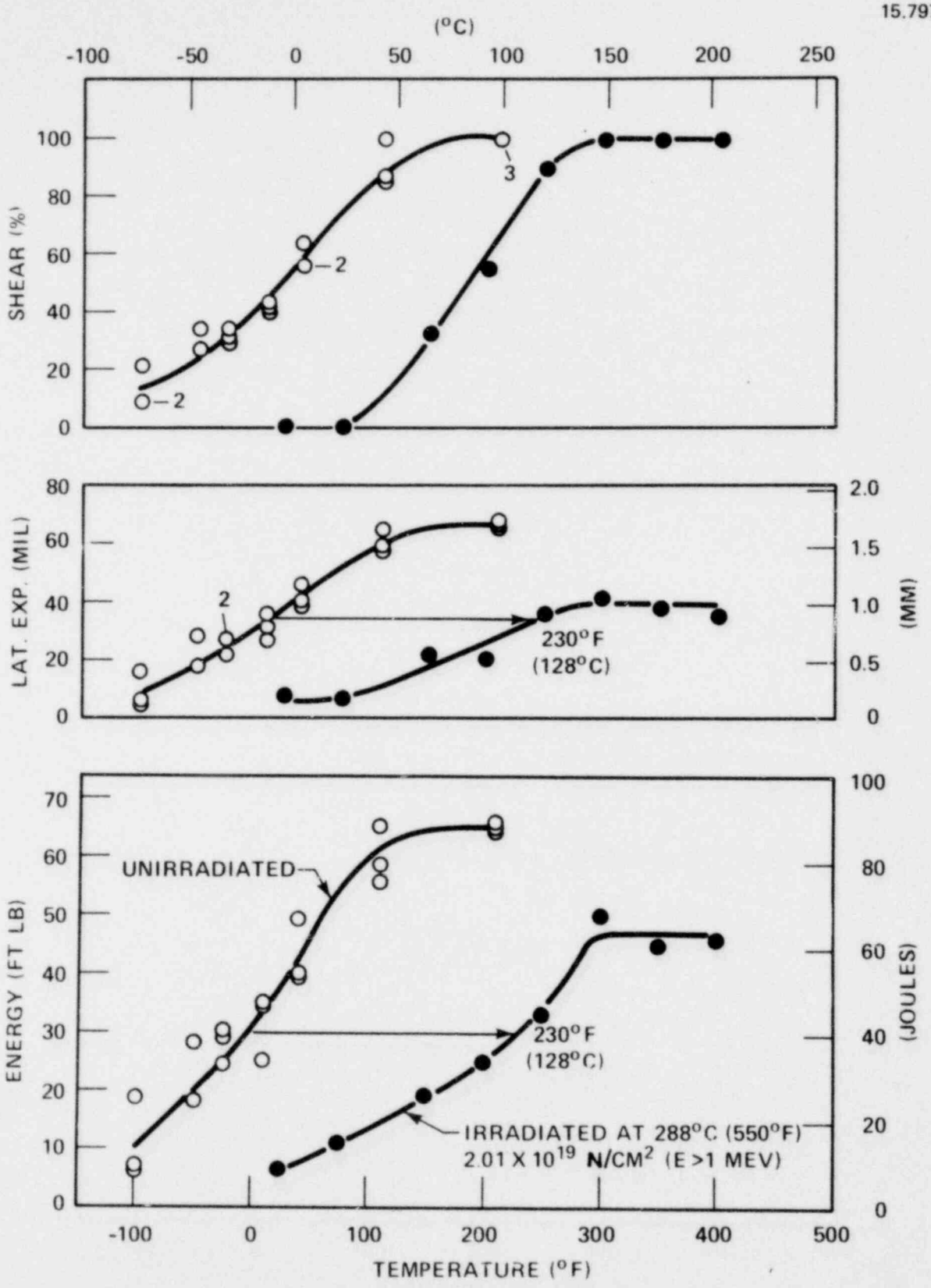

Figure 5-3. Charpy V-Notch Impact Data for the Point Beach Unit No. 2 Pressure Vessel Weld Metal

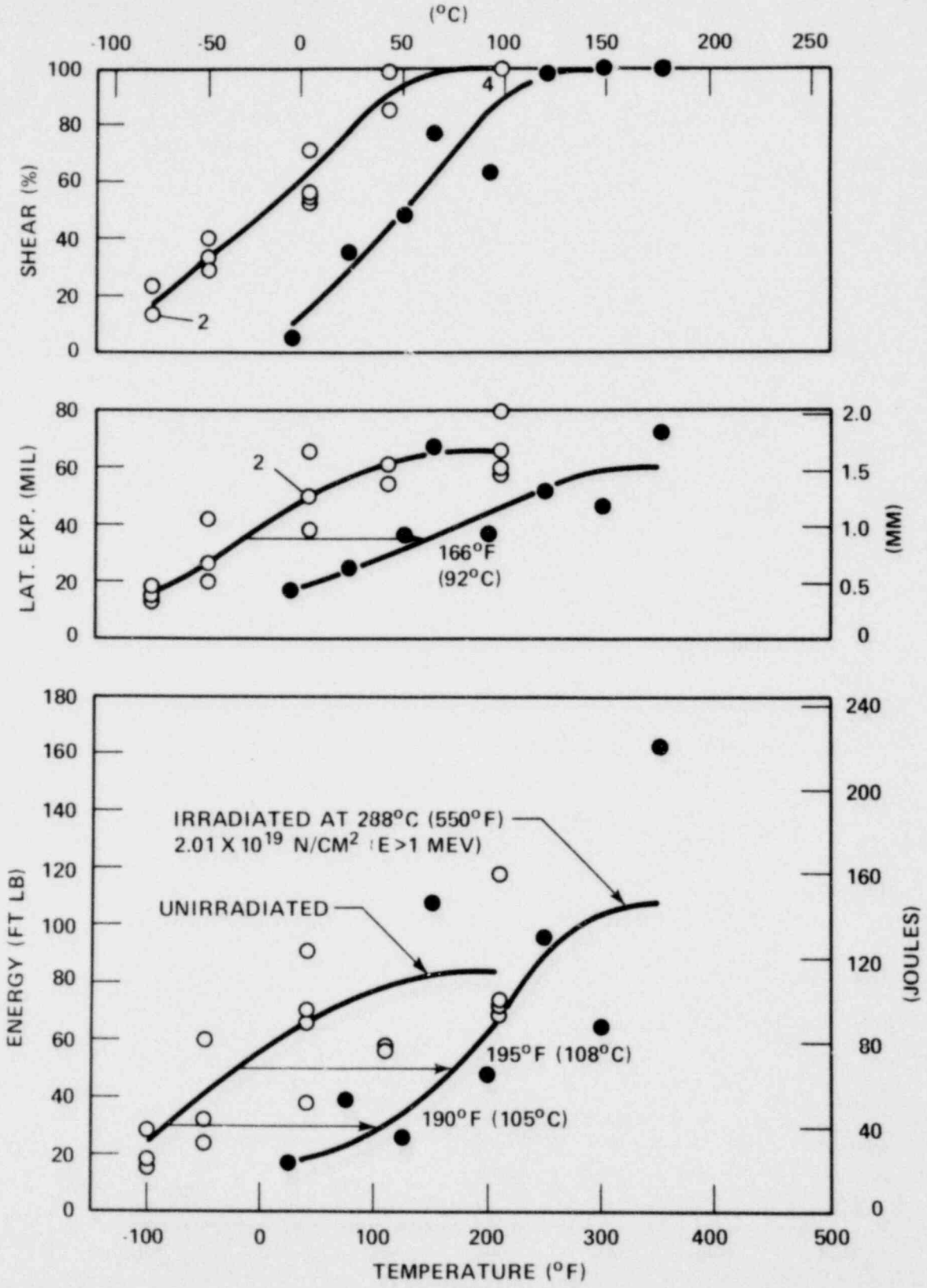

Figure 5-4. Charpy V-Notch Impact Data for the Point Beach Unit No. 2 Weld Heat-Affected-Zone Metal

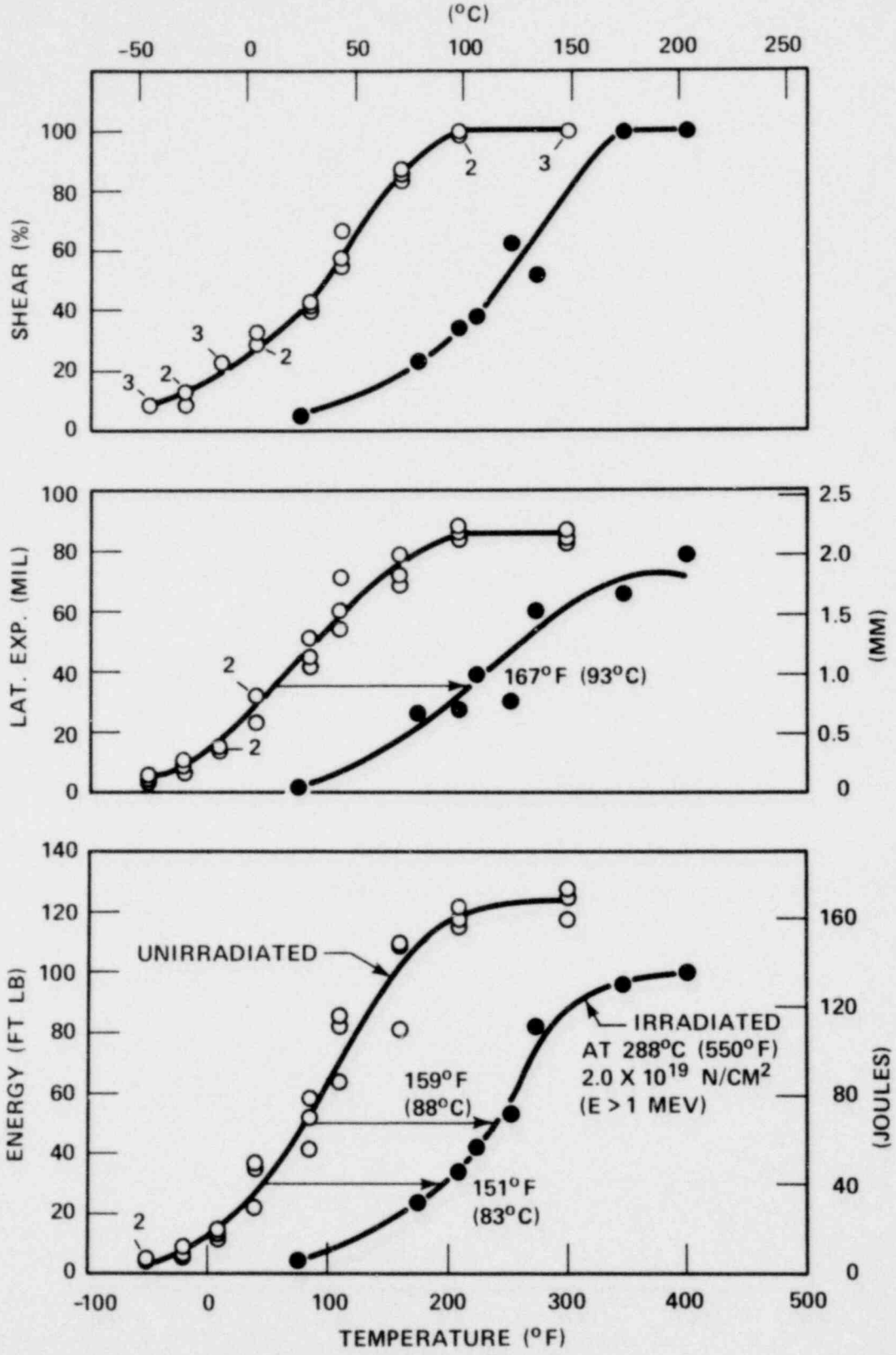

Figure 5-5. Charpy V-Notch Impact Data for A533 Grade B Class 1 ASTM Correlation Monitor Material

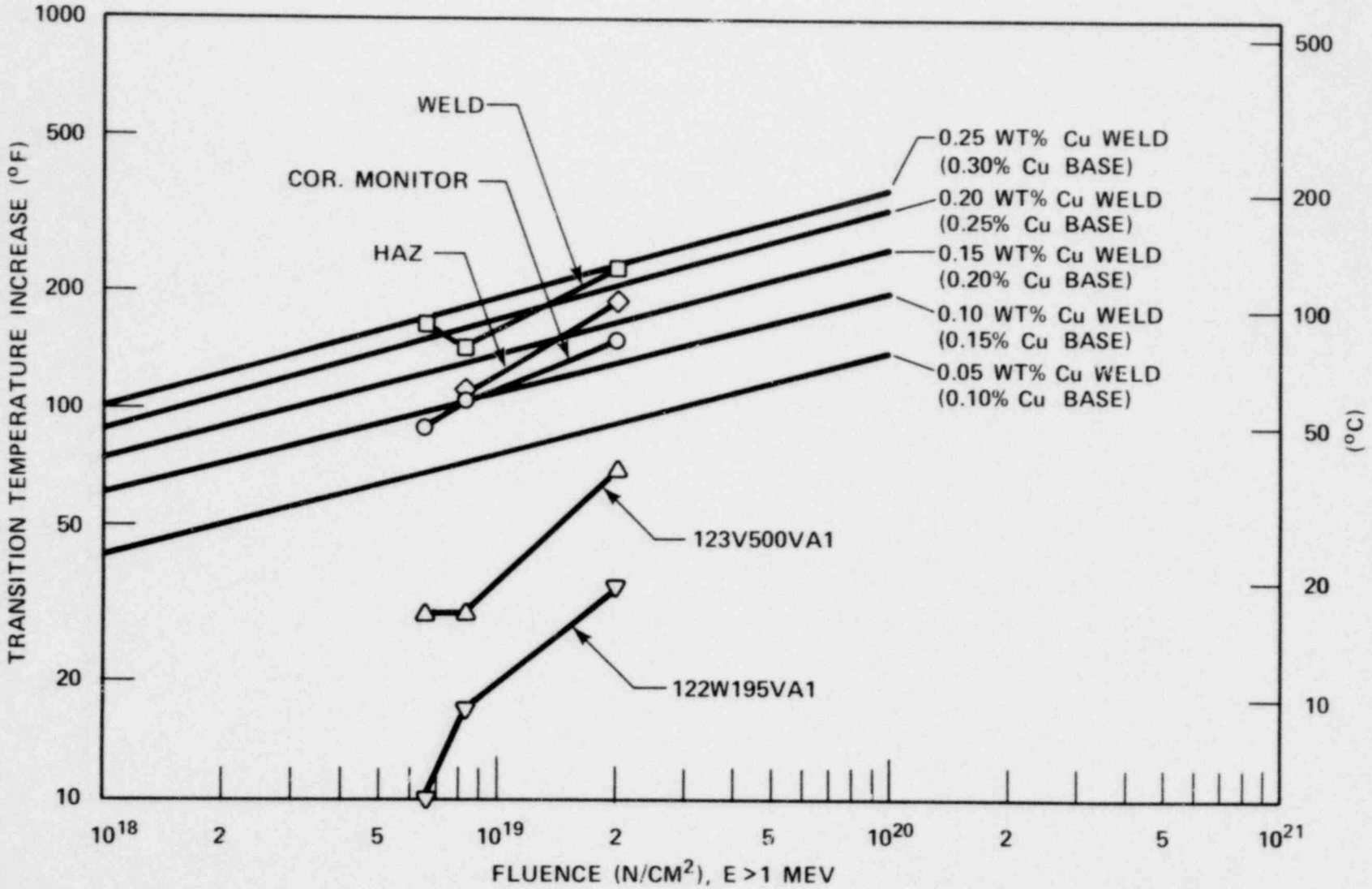

Figure 5-6. Point Beach Unit No. 2 Material 30 ft lb Transition Temperature Increases as Compared to Westinghouse Predictions

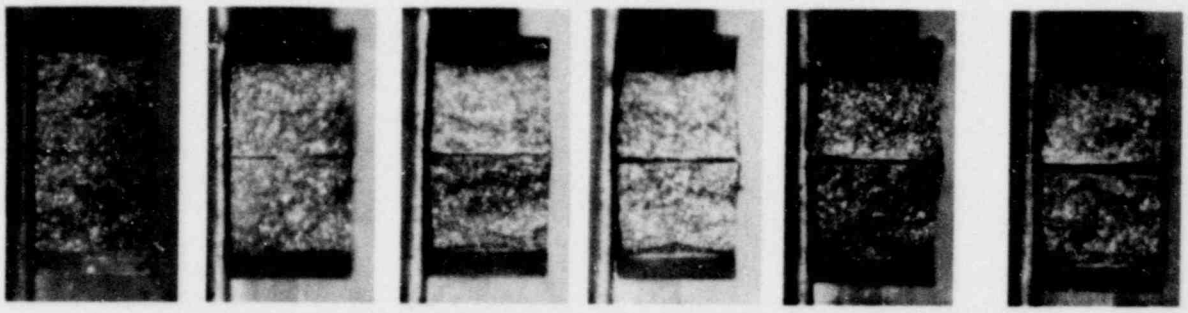

V23 V14 V24 V21 V20 V22

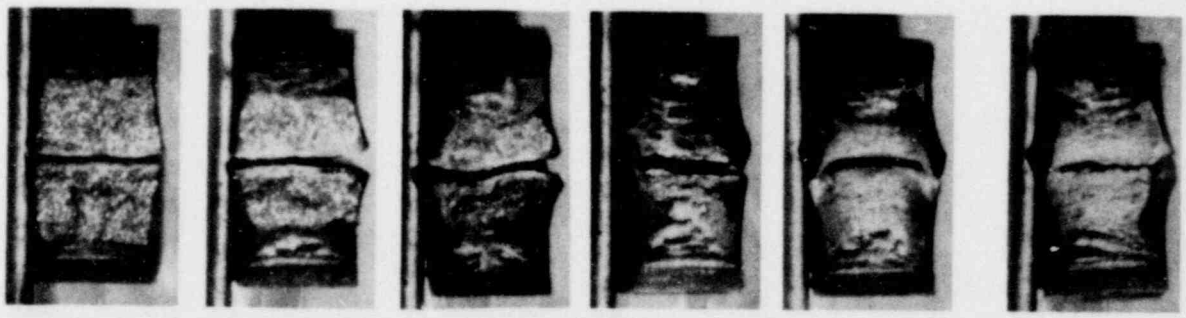

V17 V16 V13 V15 V19 V18

Figure 5-7. Charpy Impact Specimen Fracture Surfaces for Point Beach Unit No. 2 Pressure Vessel Intermediate Shell Forging 123V500VA1

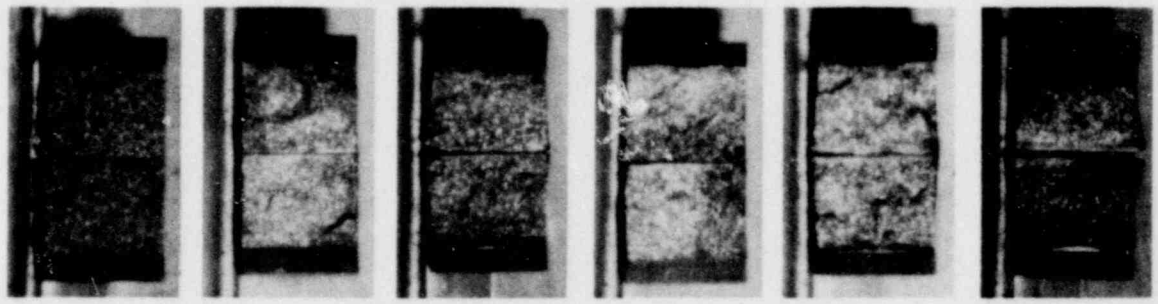

E20 E24 E17 E18 E14 E22

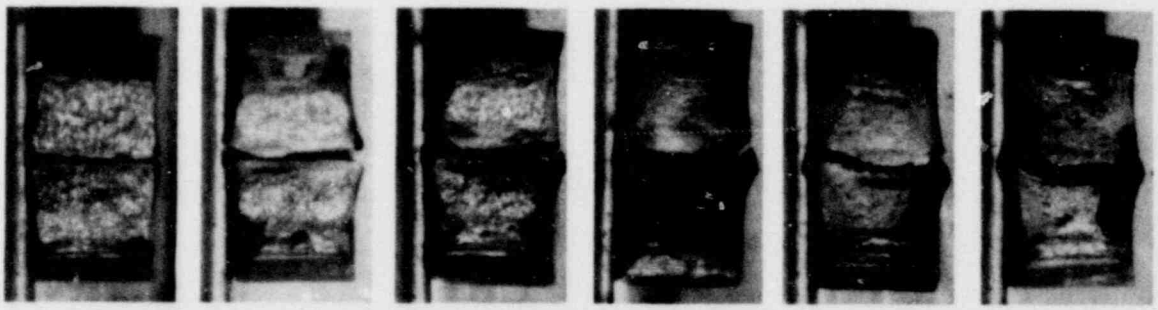

E23 E13 E21 E16 E15 E19

Figure 5-8. Charpy Impact Specimen Fracture Surfaces for Point Beach Unit No. 2 Pressure Vessel Lower Shell Forging 122W195VA1

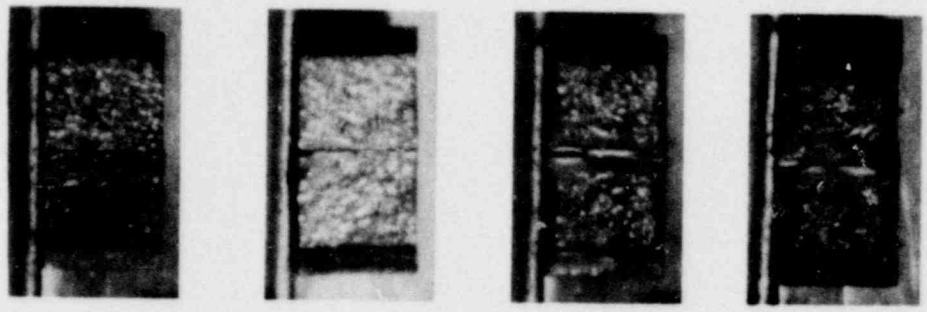

W11 W16 W9 W12

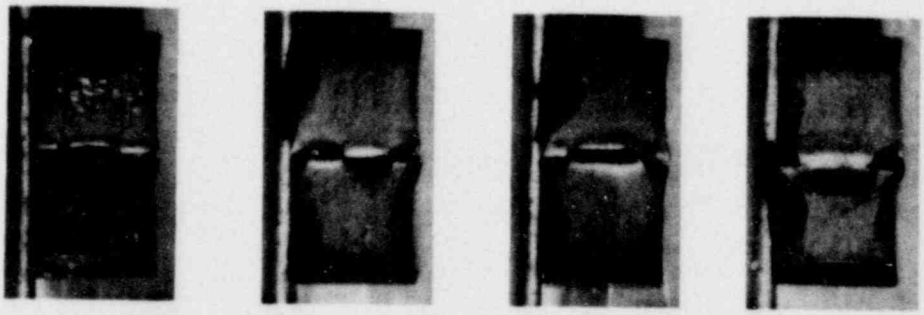

W15 W10 W14 W13

Figure 5-9. Charpy Impact Specimen Fracture Surfaces for Point Beach Unit 2 Weld Metal

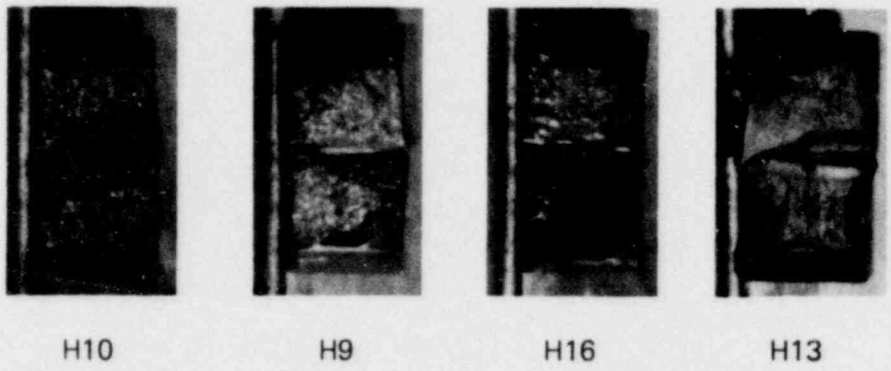

Figure 5-10. Charpy Impact Specimen Fracture Surfaces for Point Beach Unit No. 2 Weld Heat-Affected-Zone Metal

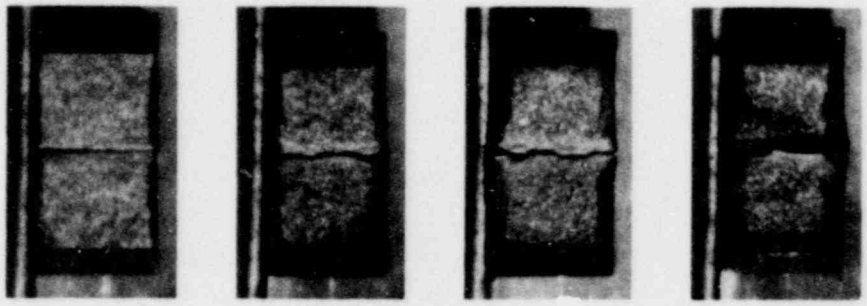

R14 R12 R13 R11

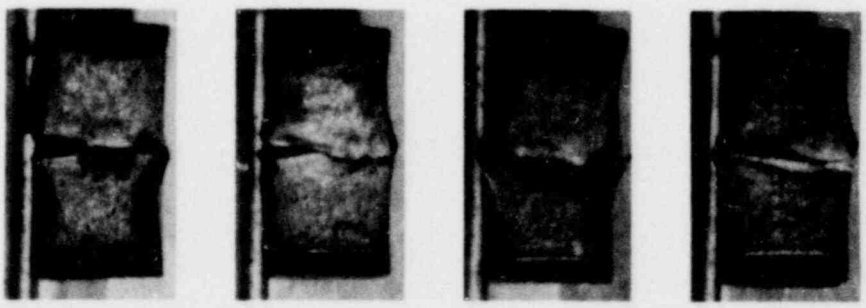

R10 R9 R15 R16

Figure 5-11. Charpy Impact Specimen Fracture Surfaces for Point Beach Unit No. 2 ASTM Correlation Monitor Material

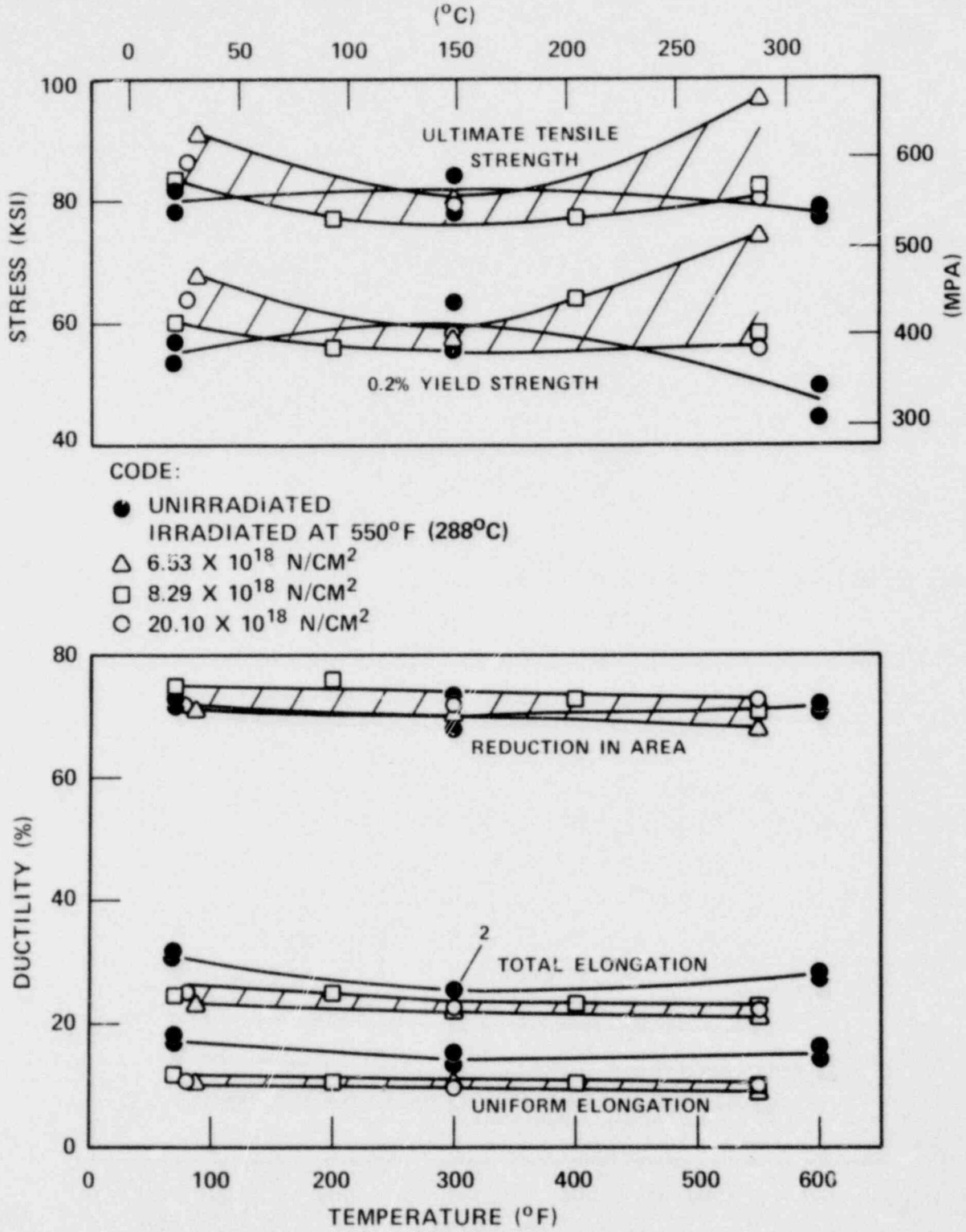

Figure 5-12. Tensile Properties for the Point Beach Unit No. 2 Pressure Vessel Intermediate Shell Forging 123V500VA1

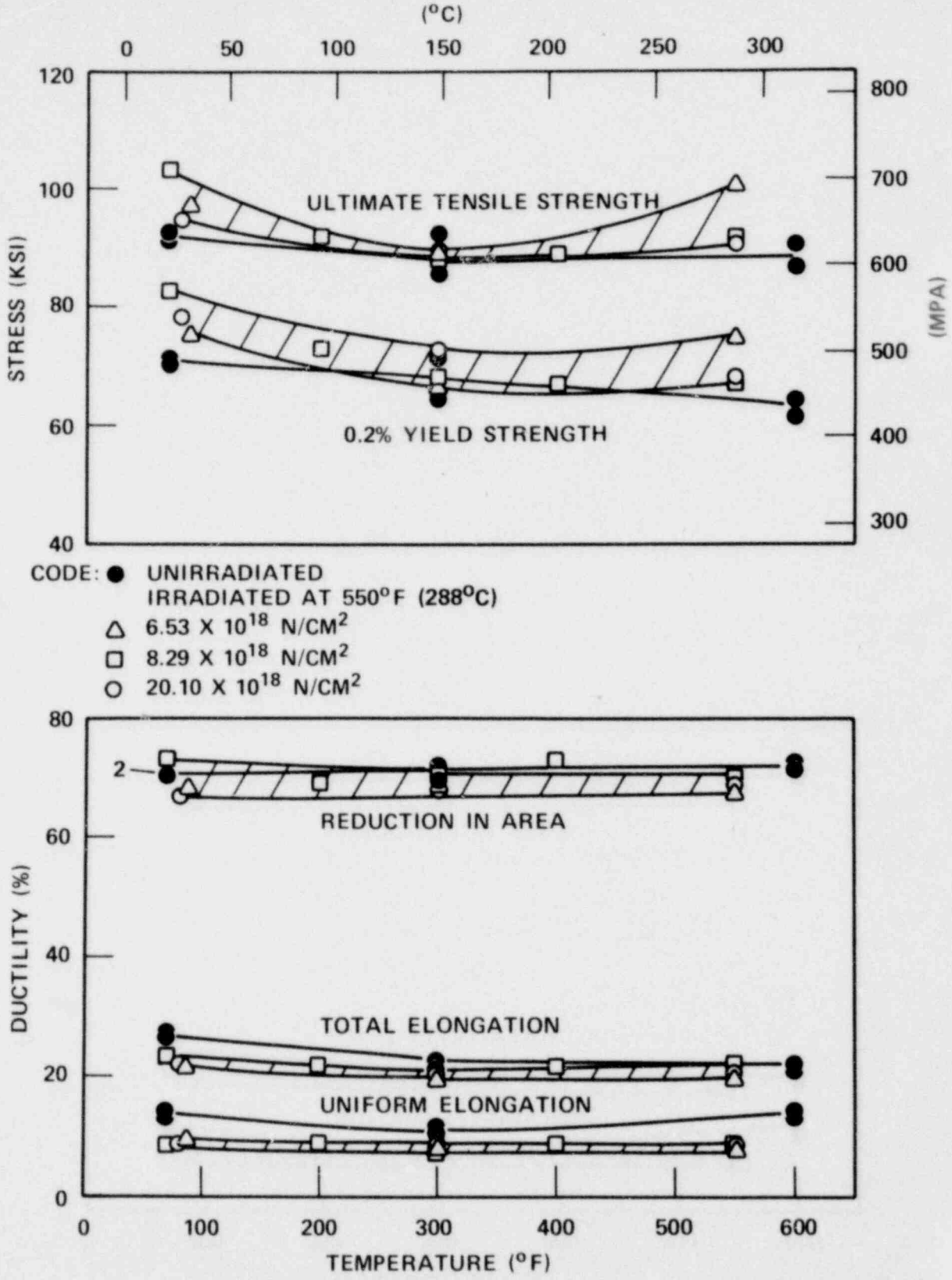

Figure 5-13. Tensile Properties for the Point Beach Unit No. 2 Pressure Vessel Lower Shell Forging 122W195VA1

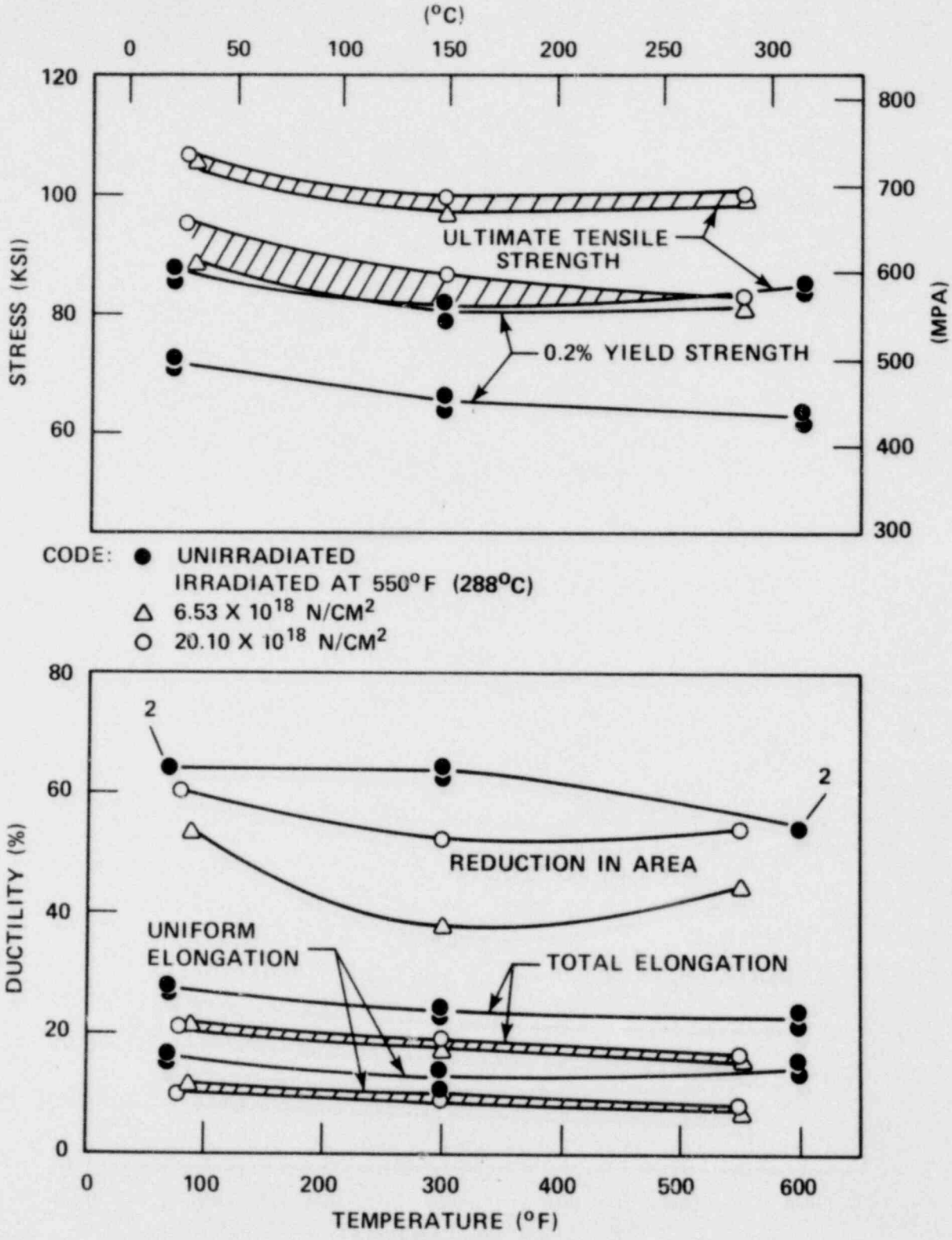

Figure 5-14. Tensile Properties for the Point Beach Unit No. 2 Pressure Vessel Weld Metal

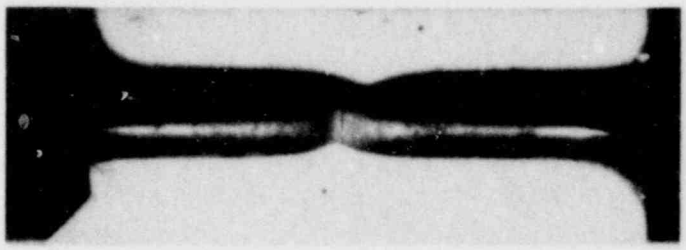

V4 27°C

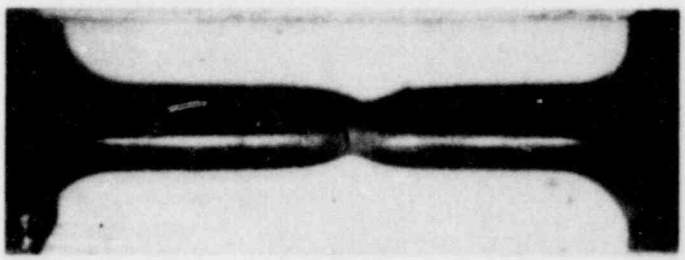

V5 149°C

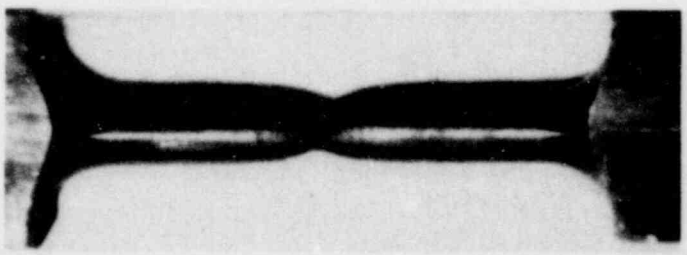

V6 288°C

Figure 5-15. Fractured Tensile Specimens from Point Beach Unit No. 2 Pressure Vessel Intermediate Shell Forging 123V500VA1

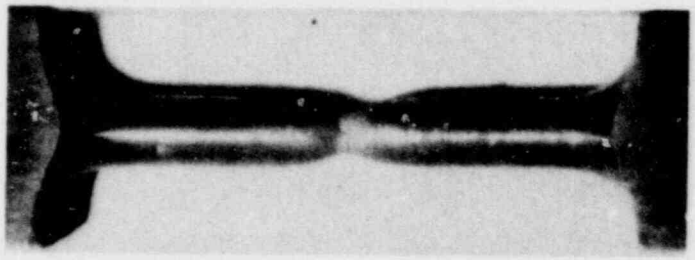

E4 27°C

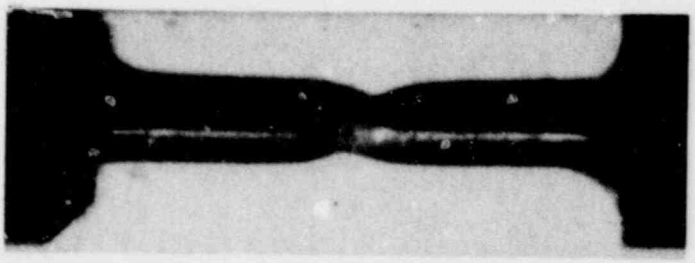

E5 149°C

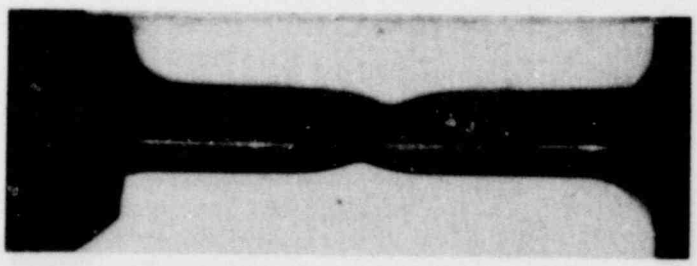

E6 288°C

Figure 5-16. Fractured Tensile Specimens from Point Beach Unit No. 2 Pressure Vessel Lower Shell Forging 122W195VA1

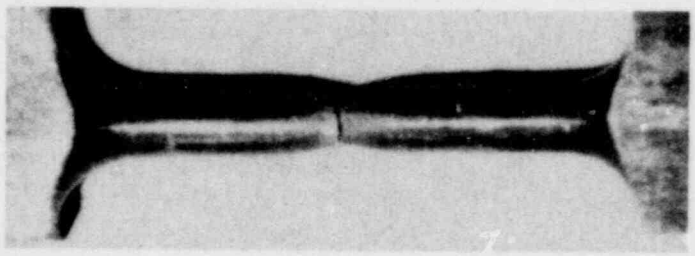

W4 27°C

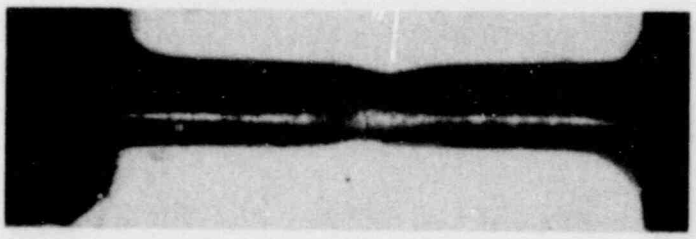

W5 149°C

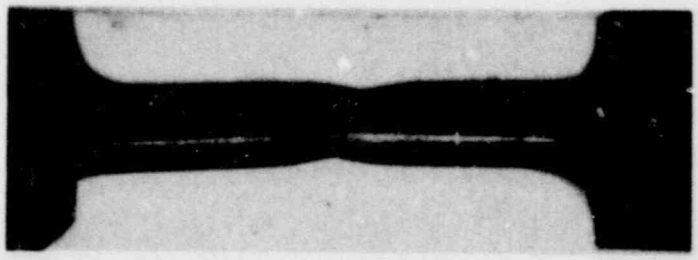

W6 288°C

Figure 5-17. Fractured Tensile Specimens from Point Beach Unit No. 2 Pressure Vessel Weld Metal

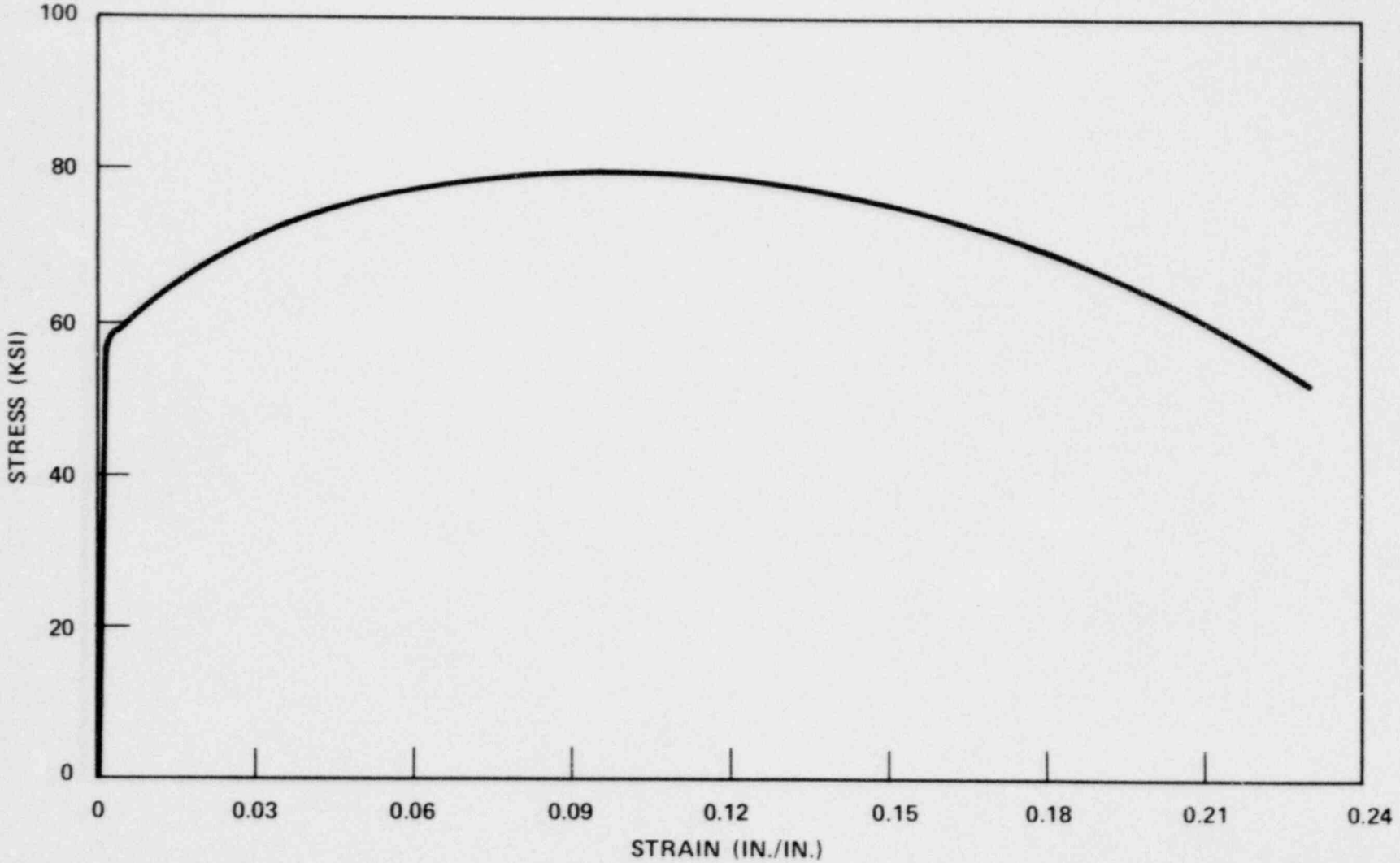

Figure 5-18. Typical Stress Strain Curve for Tension Specimens (Tension Specimen No. V5)

SECTION 6
RADIATION ANALYSIS AND NEUTRON DOSIMETRY

6-1. INTRODUCTION

Knowledge of the neutron environment within the pressure vessel-surveillance capsule geometry is required as an integral part of LWR pressure vessel surveillance programs for two reasons. First, in the interpretation of radiation-induced property changes observed in materials test specimens, the neutron environment (fluence, flux) to which the test specimens were exposed must be known. Second, in relating the changes observed in the test specimens to the present and future condition of the reactor pressure vessel, a relationship between the environment at various positions within the reactor vessel and that experienced by the test specimens must be established. The former requirement is normally met by employing a combination of rigorous analytical techniques and measurements obtained with passive neutron flux monitors contained in each of the surveillance capsules. The latter information, on the other hand, is derived solely from analysis.

This section describes a discrete ordinates Sn transport analysis performed for the Point Beach Unit 2 reactor to determine the fast neutron (E> 1.0 Mev) flux and fluence as well as the neutron energy spectra within the reactor vessel and surveillance capsules; and, in turn, to develop lead factors for use in relating neutron exposure of the pressure vessel to that of the surveillance capsules. Based on spectrum-averaged reaction cross sections derived from this calculation, the analysis of the neutron dosimetry contained in Capsule R is discussed and updated evaluations of dosimetry from Capsules V and T are presented.

6-2. DISCRETE ORDINATES ANALYSIS

A plan view of the Point Beach reactor geometry at the core midplane is shown in figure 6-1. Since the reactor exhibits 1/8th core symmetry, only a 0°-45° sector is depicted. Six irradiation capsules attached to the thermal shield are included in the design to constitute the reactor vessel surveillance program. Two capsules are located symmetrically at 13°, 23°, and 33° from the cardinal axis as shown in figure 6-1.

A plan view of a single surveillance capsule attached to the thermal shield is shown in figure 6-2. The stainless steel specimen container is 1-inch square and approximately 63 inches in height. The containers are positioned axially such that the specimens are centered on the core midplane, thus spanning the central 5.25 feet of the 12-foot-high reactor core.

From a neutronic standpoint, the surveillance capsule structures are significant. In fact, as will be shown later, they have a marked impact on the distributions of neutron flux and energy spectra in the water annulus between the thermal shield and the reactor vessel. Thus, in order to properly ascertain the neutron environment at the test specimen locations, the capsules themselves must be included in the analytical model. Use of at least a two-dimensional computation is, therefore, mandatory.

In the analysis of the neutron environment within the Point Beach Unit 2 reactor geometry, predictions of neutron flux magnitude and energy spectra were made with the DOT[5] two-dimensional discrete ordinates code. The radial and azimuthal distributions were obtained from an R, Θ computation wherein the geometry shown in figures 6-1 and 6-2 was described in the analytical model. In addition to the R, Θ computation, a second calculation in R, Z geometry was also carried out to obtain relative axial variations of neutron flux throughout the geometry of interest. In the R, Z analysis the reactor core was treated as an equivalent volume cylinder and, of course, the surveillance capsules were not included in the model.

Both the R, Θ and the R, Z analyses employed 21 neutron energy groups, an S_8 angular quadrature, and a P_1 cross-section expansion. The cross sections were generated via the Westinghouse GAMBIT[6] code system with broad group processing by the APPROPOS[7] and ANISN[8] codes. The energy group structure used in the analysis is listed in table 6-1.

A key input parameter in the analysis of the integrated fast neutron exposure of the reactor vessel is the core power distribution. For the analysis, power distributions representative of time-averaged conditions derived from statistical studies of long-term operation of Westinghouse two-loop plants were employed. These input distributions include rod-by-rod spatial variations for all peripheral fuel assemblies.

It should be noted that this particular power distribution is intended to produce accurate end-of-life neutron exposure levels for the pressure vessel. As such, the calculation is indeed representative of an average neutron flux and small (± 15-20%) deviations from cycle to cycle are to be expected.

TABLE 6-1
21 GROUP ENERGY STRUCTURE

Group	Lower Energy (Mev)
1	7.79*
2	6.07
3	4.72
4	3.68
5	2.87
6	2.23
7	1.74
8	1.35
9	1.05
10	0.821
11	0.388
12	0.111
13	4.09×10^{-2}
14	1.50×10^{-2}
15	5.53×10^{-3}
16	5.83×10^{-4}
17	7.89×10^{-5}
18	1.07×10^{-5}
19	1.86×10^{-6}
20	3.00×10^{-7}
21	0.0

*Upper energy of group 1 is 10.0 Mev

Having the results of the R,Θ and R,Z calculations, three-dimensional variations of neutron flux may be approximated by assuming that the following relation holds for the applicable regions of the reactor.

$$\phi(R,Z,\Theta,E_g) = \phi(R,\Theta,E_g)\, F(Z,E_g) \qquad (6\text{-}1)$$

where:

$\phi(R,Z,\Theta,E_g)$ = neutron flux at point R,Z,Θ within energy group g

$\phi(R,\Theta,E_g)$ = neutron flux at point R,Θ within energy group g obtained from the R,Θ calculation

$F(Z,E_g)$ = relative axial distribution of neutron flux within energy group g obtained from the R,Z calculation

6-3. NEUTRON DOSIMETRY

The passive neutron flux monitors included in the Point Beach Unit 2 surveillance program are listed in table 6-2. The first five reactions in table 6-2 are used as fast neutron monitors to relate neutron fluence (E> 1.0 Mev) to measured materials properties changes. To properly account for burnout of the product isotope generated by fast neutron reactions, it is necessary to also determine the magnitude of the thermal neutron flux at the monitor location. Therefore, bare and cadmium-covered cobalt-aluminum monitors were also included.

The relative locations of the various monitors within the surveillance capsules are shown in figure 4-2. The nickel, copper, and cobalt-aluminum monitors, in wire form, are placed in holes drilled in spacers at several axial levels within the capsules. The iron monitors are obtained by drilling samples from selected Charpy test specimens. The cadmium-shielded neptunium and uranium fission monitors are accommodated within the dosimeter block located near the center of the capsule.

The use of passive monitors such as those listed in table 6-2 does not yield a direct measure of the energy-dependent flux level at the point of interest. Rather, the activation or fission process is a measure of the integrated effect that the time- and energy-dependent neutron flux has on the target material over the course of the irradiation period. An accurate assessment of the average neutron flux level incident on the various monitors may be derived from the activation measurements only if the irradiation parameters are well known. In particular, the following variables are of interest:

TABLE 6-2

NUCLEAR PARAMETERS FOR NEUTRON FLUX MONITORS

Monitor Material	Reaction of Interest	Target Weight Fraction	Response Range	Product Half-Life	Fission Yield (%)
Copper	$Cu^{63}(n,\alpha)Co^{60}$	0.6917	E>4.7 Mev	5.27 years	
Iron	$Fe^{54}(n,p)Mn^{54}$	0.0585	E>1.0 Mev	314 days	
Nickel	$Ni^{58}(n,p)Co^{68}$	0.6777	E>1.0 Mev	71.4 days	
Uranium-238*	$U^{238}(n,f)Cs^{137}$	1.0	E>0.4 Mev	30.2 years	6.3
Neptunium-237*	$Np^{237}(n,f)Cs^{137}$	1.0	E>0.08 Mev	30.2 years	6.5
Cobalt-Aluminum*	$Co^{59}(n,\gamma)Co^{60}$	0.0015	0.4eV<0.015Mev	5.27 years	
Cobalt-Aluminum	$Co^{59}(n,\gamma)Co^{60}$	0.0015	E<0.0015 Mev	5.27 years	

*Denotes that monitor is cadmium shielded

- The operating history of the reactor
- The energy response of the monitor
- The neutron energy spectrum at the monitor location
- The physical characteristics of the monitor

The analysis of the passive monitors and subsequent derivation of the average neutron flux requires completion of two procedures. First, the disintegration rate of product isotope per unit mass of monitor must be determined. Second, in order to define a suitable spectrum averaged reaction cross section, the neutron energy spectrum at the monitor location must be calculated.

The specific activity of each of the monitors is determined using established ASTM procedures.[9,10,11,12,13] Following sample preparation, the activity of each monitor is determined by means of a lithium-drifted germanium, Ge(Li), gamma spectrometer. The overall standard deviation of the measured data is a function of the precision of sample weighing, the uncertainty in counting, and the acceptable error in detector calibration. For the samples removed from Point Beach Unit 2, the overall 2σ deviation in the measured data is determined to be $\pm$ 10 percent. The neutron energy spectra are determined analytically using the method described in section 6-1.

Having the measured activity of the monitors and the neutron energy spectra at the locations of interest, the calculation of the neutron flux proceeds as follows.

The reaction product activity in the monitor is expressed as

$$R = \frac{N_o}{A} f_i Y \int_E \sigma(E)\phi(E) \sum_{j=1}^{N} \frac{P_j}{P_{max}} (1 - e^{-\lambda t_j}) e^{-\lambda t_d} \qquad (6\text{-}2)$$

where:

R = induced product activity

N_o = Avagadro's number

A = atomic weight of the target isotope

f_i = weight fraction of the target isotope in the target material

Y = number of product atoms produced per reaction

$\sigma(E)$ = energy-dependent reaction cross section

$\phi(E)$ = energy-dependent neutron flux at the monitor location with the reactor at full power

P_j = average core power level during irradiation period j

P_{max} = maximum or reference core power level

λ = decay constant of the product isotope

t_j = length of irradiation period j

t_d = decay time following irradiation period j

Since neutron flux distributions are calculated using multigroup transport methods and, further, since the prime interest is in the fast neutron flux above 1.0 Mev, spectrum-averaged reaction cross sections are defined such that the integral term in equation (6-2) is replaced by the following relation.

$$\int_E \sigma(E)\ \phi(E)dE \ = \ \overline{\sigma}\ \phi(E > 1.0\ \text{Mev})$$

where:

$$\bar{\sigma} = \frac{\int_{0}^{\infty} \sigma(E)\,\phi(E)\,dE}{\int_{1.0Mev}^{\infty} \phi(E)\,dE} = \frac{\sum_{G=1}^{N} \sigma_g \phi_g}{\sum_{G=G_{1.0Mev}}^{N} \phi_g}$$

Thus, equation (6-2) is rewritten

$$R = \frac{N_o}{A} f_i\, y\, \sigma\, \phi\,(E>1.0\ Mev) \sum_{j=1}^{N} \frac{P_j}{P_{max}} (1-e^{-\lambda t_j})\, e^{-\lambda t_d}$$

or, solving for the neutron flux,

$$\phi\,(E>1.0\ Mev) = \frac{R}{\frac{N_o}{A} f_i\, y\, \sigma \sum_{j=1}^{N} \frac{P_j}{P_{max}} (1-e^{-\lambda t_j})\, e^{-\lambda t_d}} \qquad (6\text{-}3)$$

The total fluence above 1.0 Mev is then given by

$$\Phi\,(E>1.0\ Mev) = \phi\,(E>1.0\ Mev) \sum_{j=1}^{N} \frac{P_j}{P_{max}} t_j \qquad (6\text{-}4)$$

where:

$\sum_{j=1}^{N} \frac{P_j}{P_{max}}$ t_j = total effective full power seconds of reactor operation up to the time of capsule removal

An assessment of the thermal neutron flux levels within the surveillance capsules is obtained from the bare and cadmium-covered $Co^{59}(n,\delta)Co^{60}$ data by means of cadmium ratios and the use of a 37-barn 2200 m/sec cross section. Thus,

$$\phi_{Th} = \frac{R_{bare} \left\{ \frac{D-1}{D} \right\}}{\frac{N_o}{A} f_i y\sigma \sum_{j=1}^{N} \frac{P_j}{P_{max}} (1-e^{-\lambda t_j}) e^{-\lambda t_d}} \qquad (6\text{-}5)$$

where:

D is defined as $\frac{R_{bare}}{R_{Cd\ covered}}$

6-4. TRANSPORT ANALYSIS RESULTS

Results of the S_n transport calculations for the Point Beach Unit 2 reactor are summarized in figures 6-3 through 6-8 and in tables 6-3 through 6-5. In figure 6-3, the calculated maximum neutron flux levels at the surveillance capsule centerline, pressure vessel inner radius, 1/4 thickness location, and 3/4 thickness location are presented as a function of azimuthal angle. The influence of the surveillance capsules on the fast neutron flux distribution is clearly evident. In figure 6-4, the radial distribution of maximum fast neutron flux (E> 1.0Mev) through the thickness of the reactor pressure vessel is shown. The relative axial variation of neutron flux within the vessel is given in figure 6-5. Absolute axial variations of fast neutron flux may be obtained by multiplying the levels given in figures 6-3 or 6-4 by the appropriate values from figure 6-5.

In figure 6-6 the radial variations of fast neutron flux within surveillance capsules V, R, and T are presented. These data, in conjunction with the maximum vessel flux, are used to develop lead factors for each of the capsules. Here the lead factor is defined as the ratio of the fast neutron flux (E>1.0 Mev) at the dosimeter block location (capsule center) to

TABLE 6-3

CALCULATED FAST NEUTRON FLUX (E > 1.0 MEV) AND LEAD FACTORS FOR POINT BEACH UNIT NO. 2 SURVEILLANCE CAPSULES

Capsule Identification	Azimuthal Location	ϕ (E>1.0 Mev) (n/cm^2-sec)	Lead Factor
V	13°	1.33×10^{11}	3.37
R	13°	1.33×10^{11}	3.37
T	23°	7.66×10^{10}	1.94
P	23°	7.66×10^{10}	1.94
S	33°	7.06×10^{10}	1.79
N	33°	7.06×10^{10}	1.79

TABLE 6-4

CALCULATED NEUTRON ENERGY SPECTRA AT THE DOSIMETER BLOCK LOCATION FOR POINT BEACH UNIT NO. 2 SURVEILLANCE CAPSULES

Group No.	Neutron Flux (n/cm^2-sec)		
	Capsules V&R	Capsules T&P	Capsules S&N
1	7.52×10^8	5.51×10^8	4.84×10^8
2	2.47×10^9	1.83×10^9	1.61×10^9
3	4.08×10^9	2.83×10^9	2.51×10^9
4	4.58×10^9	2.93×10^9	2.65×10^9
5	7.97×10^9	4.78×10^9	4.37×10^9
6	1.56×10^{10}	9.29×10^9	8.52×10^9
7	2.26×10^{10}	1.30×10^{10}	1.20×10^{10}
8	3.25×10^{10}	1.81×10^{10}	1.68×10^{10}
9	4.30×10^{10}	2.33×10^{10}	2.16×10^{10}
10	4.64×10^{10}	2.46×10^{10}	2.28×10^{10}
11	1.54×10^{11}	7.97×10^{10}	7.39×10^{10}
12	1.94×10^{11}	9.68×10^{10}	8.98×10^{10}
13	8.67×10^{10}	4.28×10^{10}	3.99×10^{10}
14	6.54×10^{10}	3.24×10^{10}	3.02×10^{10}
15	5.22×10^{10}	2.58×10^{10}	2.41×10^{10}
16	1.21×10^{11}	5.90×10^{10}	5.51×10^{10}
17	9.52×10^{10}	4.66×10^{10}	4.35×10^{10}
18	9.75×10^{10}	4.73×10^{10}	4.43×10^{10}
19	7.74×10^{10}	3.76×10^{10}	3.52×10^{10}
20	8.59×10^{10}	4.16×10^{10}	3.89×10^{10}
21	2.73×10^{11}	1.39×10^{11}	1.25×10^{11}

TABLE 6-5

SPECTRUM AVERAGED REACTION CROSS SECTIONS AT THE DOSIMETER BLOCK LOCATION FOR POINT BEACH UNIT NO. 2 SURVEILLANCE CAPSULES

Reaction	$\bar{\sigma}$ (barns)		
	Capsules V&R	Capsules T&P	Capsules S&N
Fe^{54} (n,p) Mn^{54}	0.0595	0.0683	0.0666
Ni^{58} (n,p) Co^{58}	0.0811	0.0912	0.0893
Cu^{63} (n,α) Co^{60}	0.000404	0.000517	0.000494
U^{238} (n,f) F.P.	0.333	0.345	0.344
Np^{237} (n,f) F.P.	2.93	2.80	2.82

$$\bar{\sigma} = \frac{\int_{0}^{\infty} \sigma(E)\phi(E)dE}{\int_{1\ Mev}^{\infty} \phi(E)dE}$$

the maximum fast neutron flux at the pressure vessel inner radius. Updated lead factors for all of the Point Beach Unit 2 surveillance capsules are listed in table 6-3.

Since the neutron flux monitors contained within the surveillance capsules are not all located at the same radial location, the measured disintegration rates are analytically adjusted for the gradients that exist within the capsules so that flux and fluence levels may be derived on a common basis at a common location. This point of comparison was chosen to be the capsule center. Analytically determined reaction rate gradients for use in the adjustment procedures are shown in figures 6-7 and 6-8 for Capsules V, R, and T. All of the applicable fast neutron reactions are included.

In order to derive neutron flux and fluence levels from the measured disintegration rates, suitable spectrum-averaged reaction cross sections are required. The neutron energy spectrum calculated to exist at the center of each of the Point Beach Unit 2 surveillance capsules is given in table 6-4. The associated spectrum-averaged cross sections for each of the five fast neutron reactions are given in table 6-5.

6-5. DOSIMETRY RESULTS

The irradiation history of the Point Beach Unit 2 reactor is given in table 6-6. The data were obtained from the Point Beach semiannual operating reports.[14] Comparisons of measured and calculated saturated activity of the flux monitors contained in Capsules R, V, and T are listed in tables 6-7, 6-8, and 6-9, respectively. The data are presented as measured at the actual monitor locations as well as adjusted to the capsule center. The measured results for both capsules R and T were obtained by Westinghouse, whereas those for Capsule V were derived from reference 9. All adjustments to the capsule center were based on the data presented in figures 6-7 and 6-8.

The fast neutron (E> 1.0 Mev) flux and fluence levels derived for Capsules R, V and T are presented in table 6-10. The thermal neutron flux obtained from the cobalt-aluminum monitors is summarized in table 6-11. Due to the relatively low thermal neutron flux at the capsule locations, no burnup correction was made to any of the measured activities. The maximum error introduced by this assumption is estimated to be less than 1 percent for the Ni^{58} (n,p) Co^{58} reaction and even less significant for all of the other fast neutron reactions.

Using the iron data presented in table 6-10, along with the lead factors given in table 6-3, the fast neutron fluence (E> 1.0 Mev) for Capsules V, T, and R as well as for the reactor vessel inner diameter are summarized in table 6-12 and figure 6-9. The agreement between calculation and measurement is excellent, with measured fluence levels of 6.53×10^{18}, 8.29×10^{18}, and 2.01×10^{19} compared to calculated values of

TABLE 6-6

IRRADIATION HISTORY OF POINT BEACH UNIT NO. 2
REACTOR VESSEL SURVEILLANCE CAPSULES

Month	P_J (MW)	P_{max} (MW)	$\frac{P_J}{P_{max}}$	Irradiation Time (days)	Decay * Time (days)
10/72-12/72	369	1518	.243	92	2357
1/73	284	1518	.187	31	2326
2/73	278	1518	.183	28	2298
3/73	740	1518	.487	31	2267
4/73	743	1518	.489	30	2237
5/73	1043	1518	.687	31	2206
6/73	1300	1518	.856	30	2176
7/73	1325	1518	.873	31	2145
8/73	1397	1518	.920	31	2114
9/73	1501	1518	.989	30	2084
10/73	1474	1518	.971	31	2053
11/73	1479	1518	.974	30	2023
12/73	1424	1518	.938	31	1992
1/74	1462	1518	.963	31	1961
2/74	1458	1518	.960	28	1933
3/74	1485	1518	.978	31	1902
4/74	1495	1518	.985	30	1872
5/74	1494	1518	.984	31	1841
6/74	1229	1518	.810	30	1811
7/74	1283	1518	.845	31	1780
8/74	1494	1518	.984	31	1749
9/74	1464	1518	.964	30	1719
10/74	750	1518	.494	31	1688
CAPSULE V REMOVED					
11/74	0	1518	0	30	1658
12/74	406	1518	.267	31	1627
1/75	1497	1518	.986	31	1596
2/75	1311	1518	.864	28	1568

*Decay time is referenced to June 15, 1979.

TABLE 6-6 (cont)

IRRADIATION HISTORY OF POINT BEACH UNIT NO. 2
REACTOR VESSEL SURVEILLANCE CAPSULES

Month	P_J (MW)	Pmax (MW)	$\frac{P_J}{P_{max}}$	Irradiation Time (days)	Decay* Time (days)
3/75	1454	1518	.958	31	1537
4/75	1273	1518	.839	30	1507
5/75	1183	1518	.779	31	1476
6/75	1270	1518	.837	30	1446
7/75	1430	1518	.942	31	1415
8/75	1006	1518	.663	31	1384
9/75	1385	1518	.912	30	1354
10/75	1330	1518	.876	31	1323
11/75	1354	1518	.892	30	1293
12/75	1498	1518	.987	31	1262
1/76	1439	1518	.948	31	1231
2/76	1335	1518	.879	29	1202
3/76	155	1518	.102	31	1171
4/76	1351	1518	.890	30	1141
5/76	1286	1518	.847	31	1110
6/76	1400	1518	.922	30	1080
7/76	1380	1518	.909	31	1049
8/76	1374	1518	.905	31	1018
9/76	1397	1518	.920	30	988
10/76	1500	1518	.988	31	957
11/76	1478	1518	.974	30	927
12/76	1482	1518	.976	31	896
1/77	1482	1518	.976	31	865
2/77	1485	1518	.978	28	837
3/77	135	1518	.089	31	806
CAPSULE T REMOVED					
4/77	293	1518	.193	30	776
5/77	1506	1518	.992	31	745

*Decay time is referenced to June 15, 1979.

TABLE 6-6 (cont)

IRRADIATION HISTORY OF POINT BEACH UNIT NO. 2
REACTOR VESSEL SURVEILLANCE CAPSULES

Month	P_J (MW)	P_{max} (MW)	$\frac{P_J}{P_{max}}$	Irradiation Time (days)	Decay* Time (days)
6/77	1497	1518	.986	30	715
7/77	1454	1518	.958	31	684
8/77	1322	1518	.871	31	653
9/77	1456	1518	.959	30	623
10/77	1497	1518	.986	31	592
11/77	1472	1518	.970	30	562
12/77	1485	1518	.978	31	531
1/78	1398	1518	.921	31	500
2/78	1474	1518	.971	28	472
3/78	972	1518	.640	31	441
4/78	495	1518	.326	30	411
5/78	1500	1518	.988	31	380
6/78	1472	1518	.970	30	350
7/78	1413	1518	.931	31	319
8/78	1428	1518	.941	31	288
9/78	1474	1518	.971	30	258
10/78	1488	1518	.980	31	227
11/78	1491	1518	.982	30	197
12/78	1431	1518	.943	31	166
1/79	1480	1518	.975	31	135
2/79	1480	1518	.975	28	107
3/79	994	1518	.655	31	76

*Decay time is referenced to June 15, 1979.

TABLE 6-7

COMPARISON OF MEASURED AND CALCULATED FAST NEUTRON FLUX MONITOR SATURATED ACTIVITIES FOR CAPSULE R

Reaction and Axial Location	Radial Location (cm)	Saturated Activity (DPS/gm)		Adjusted Saturated Activity (DPS/gm)	
		Capsule R	Calculated	Capsule R	Calculated
$Fe^{54}(n,p)Mn^{54}$					
V-13	157.33	6.18×10^6	6.11×10^6	5.27×10^6	
E-23	157.33	5.72×10^6	6.11×10^6	4.88×10^6	
E-13	157.33	4.96×10^6	6.11×10^6	4.23×10^6	
H-9	158.33	4.66×10^6	4.95×10^6	4.90×10^6	
R-14	158.33	4.77×10^6	4.95×10^6	5.01×10^6	
W-16	158.33	4.61×10^6	4.95×10^6	4.84×10^6	
Average				4.86×10^6	5.20×10^6
$Cu^{63}(n,\alpha)Co^{60}$					
Top	158.33	4.28×10^5	3.39×10^5	4.48×10^5	
Mid-top	158.33	3.87×10^5	3.39×10^5	4.05×10^5	
Mid-bottom	158.33	4.28×10^5	3.39×10^5	4.48×10^5	
Bottom	158.33	4.54×10^5	3.39×10^5	4.75×10^5	
Average				4.44×10^5	3.55×10^5
$Ni^{58}(n,p)Co^{58}$					
Middle	158.33	7.45×10^7	7.30×10^7	7.86×10^7	7.70×10^7
$Np^{237}(n,f)Cs^{137}$					
Middle	158.10	6.79×10^7	6.45×10^7	6.79×10^7	6.45×10^7
$U^{238}(n,f)Cs^{137}$					
Middle	158.10	9.03×10^6	7.10×10^6	9.03×10^6	7.10×10^6

TABLE 6-8

COMPARISON OF MEASURED AND CALCULATED FAST NEUTRON FLUX MONITOR SATURATED ACTIVITIES FOR CAPSULE V

Reaction and Axial Location	Radial Location (cm)	Saturated Activity (DPS/gm)		Adjusted Saturated Activity (DPS/gm)	
		Capsule V	Calculated	Capsule V	Calculated
$Fe^{54}(n,p)Mn^{54}$					
Top	158.33	5.12×10^6	4.95×10^6	5.38×10^6	
Mid-top	158.33	4.87×10^6	4.95×10^6	5.12×10^6	
Middle	158.33	4.74×10^6	4.95×10^6	4.98×10^6	
Mid-bottom	158.33	5.49×10^6	4.95×10^6	5.77×10^6	
Bottom	158.33	4.90×10^6	4.95×10^6	5.15×10^6	
Average				5.28×10^6	5.20×10^6
$Cu^{63}(n,\alpha)Co^{60}$					
Top	158.33	3.99×10^5	3.39×10^5	4.18×10^5	
Mid-top	158.33	3.75×10^5	3.39×10^5	3.93×10^5	
Mid-bottom	158.33	4.09×10^5	3.39×10^5	4.28×10^5	
Bottom	158.33	4.14×10^5	3.39×10^5	4.34×10^5	
Average				4.18×10^5	3.55×10^5
$Ni^{58}(n,p)Co^{58}$					
Middle	158.33	5.84×10^7	7.30×10^7	6.16×10^7	7.70×10^7
$Np^{237}(n,f)Cs^{137}$					
Middle	158.10	6.58×10^7	6.45×10^7	6.58×10^7	6.45×10^7
$U^{238}(n,f)Cs^{137}$					
Middle	158.10	9.29×10^6	7.10×10^6	9.29×10^6	7.10×10^6

TABLE 6-9

COMPARISON OF MEASURED AND CALCULATED FAST NEUTRON FLUX MONITOR SATURATED ACTIVITIES FOR CAPSULE T

Reaction and Axial Location	Radial Location (cm)	Saturated Activity (DPS/gm)		Adjusted Saturated Activity (DPS/gm)	
		Capsule T	Calculated	Capsule T	Calculated
$Fe^{54}(n,p)Mn^{54}$					
E-47	157.33	4.07×10^6	4.05×10^6	3.43×10^6	
V-37	157.33	3.99×10^6	4.05×10^6	3.36×10^6	
E-37	157.33	3.90×10^6	4.05×10^6	3.28×10^6	
W-32	158.33	3.31×10^6	3.29×10^6	3.43×10^6	
H-25	158.33	3.48×10^6	3.29×10^6	3.61×10^6	
R-30	158.33	3.14×10^6	3.29×10^6	3.25×10^6	
Average				3.39×10^6	3.41×10^6
$Cu^{63}(n,\alpha)Co^{60}$					
Top	158.33	2.99×10^5	2.52×10^5	3.17×10^5	
Mid-top	158.33	2.70×10^5	2.52×10^5	2.86×10^5	
Mid-bottom	158.33	3.12×10^5	2.52×10^5	3.31×10^5	
Bottom	158.33	3.38×10^5	2.52×10^5	3.58×10^5	
Average				3.23×10^5	2.67×10^5
$Ni^{58}(n,p)Co^{58}$					
Middle	158.33	4.79×10^7	4.70×10^7	5.05×10^7	4.95×10^7
$Np^{237}(n,f)Cs^{137}$					
Middle	158.10	3.84×10^7	3.40×10^7	3.84×10^7	3.40×10^7
$U^{238}(n,f)Cs^{137}$					
Middle	158.10	5.01×10^6	4.23×10^6	5.01×10^6	4.23×10^6

TABLE 6-10

RESULTS OF FAST NEUTRON DOSIMETRY FOR CAPSULES R, V, AND T

Capsule	Reaction	Adjusted Saturated Activity (DPS/gm)		ϕ(E>1.0 Mev) (n/cm^2-sec)		ϕ(E>1.0 Mev) (n/cm^2)	
		Measured	Calculated	Measured	Calculated	Measured	Calculated
R	$Fe^{54}(n,p)Mn^{54}$	4.86×10^6	5.20×10^6	1.25×10^{11}	1.33×10^{11}	2.01×10^{19}	2.14×10^{19}
	$Cu^{63}(n,\alpha)Co^{60}$	4.44×10^5	3.55×10^5	1.66×10^{11}		2.67×10^{19}	
	$Ni^{58}(n,p)Co^{58}$	7.86×10^7	7.70×10^7	1.38×10^{11}		2.22×10^{19}	
	$Np^{237}(n,f)Cs^{137}$	6.79×10^7	6.45×10^7	1.40×10^{11}		2.25×10^{19}	
	$U^{238}(n,f)Cs^{137}$	9.03×10^6	7.10×10^6	1.70×10^{11}		2.74×10^{19}	
V	$Fe^{54}(n,p)Mn^{54}$	5.28×10^6	5.20×10^6	1.36×10^{11}	1.33×10^{11}	6.53×10^{18}	6.38×10^{18}
	$Cu^{63}(n,\alpha)Co^{60}$	4.18×10^5	3.55×10^5	1.56×10^{11}		7.49×10^{18}	
	$Ni^{58}(n,p)Co^{58}$	6.16×10^7	7.70×10^7	1.08×10^{11}		5.18×10^{18}	
	$Np^{237}(n,f)Cs^{137}$	6.58×10^7	6.45×10^7	1.36×10^{11}		6.53×10^{18}	
	$U^{238}(n,f)Cs^{137}$	9.29×10^6	7.10×10^6	1.75×10^{11}		8.40×10^{18}	
T	$Fe^{54}(n,p)Mn^{54}$	3.39×10^6	3.41×10^6	7.61×10^{10}	7.66×10^{10}	8.29×10^{18}	8.35×10^{18}
	$Cu^{63}(n,\alpha)Co^{60}$	3.23×10^5	2.67×10^5	9.45×10^{10}		1.03×10^{19}	
	$Ni^{58}(n,p)Co^{58}$	5.05×10^7	4.95×10^7	7.87×10^{10}		8.58×10^{18}	
	$Np^{237}(n,f)Cs^{137}$	3.84×10^7	3.40×10^7	8.30×10^{10}		9.05×10^{18}	
	$U^{238}(n,f)Cs^{137}$	5.01×10^6	4.23×10^6	9.11×10^{10}		9.93×10^{18}	

TABLE 6-11

RESULTS OF THERMAL NEUTRON DOSIMETRY FOR CAPSULES R, V, AND T

Capsule	Axial Location	Saturated Activity (dps/gm)		ϕTh (n/cm^2-sec)
		Bare	Cd-covered	
R	Top	1.77×10^8	6.88×10^7	1.91×10^{11}
	Mid-top	1.23×10^8	6.64×10^7	1.00×10^{11}
	Middle	1.30×10^8	6.40×10^7	1.17×10^{11}
	Mid-bottom	–	7.63×10^7	–
	Bottom	1.72×10^8	7.23×10^7	1.77×10^{11}
V	Top	1.40×10^8	6.25×10^7	1.37×10^{11}
	Mid-top	1.25×10^8	5.87×10^7	1.17×10^{11}
	Middle	1.01×10^8	5.18×10^7	8.68×10^{10}
	Mid-bottom	1.23×10^8	5.87×10^7	1.13×10^{11}
	Bottom	1.25×10^8	5.39×10^7	1.25×10^{11}
T	Top	1.06×10^8	–	–
	Mid-top	6.59×10^7	3.31×10^7	5.79×10^{10}
	Middle	6.85×10^7	3.51×10^7	5.90×10^{10}
	Mid-bottom	8.59×10^7	3.84×10^7	8.41×10^{10}
	Bottom	8.13×10^7	3.67×10^7	7.87×10^{10}

TABLE 6-12

SUMMARY OF NEUTRON DOSIMETRY RESULTS FOR CAPSULES V, T, AND R

Capsule	Irradiation Time (EFPS)	ϕ(E>1.0 Mev) (n/cm^2-sec)	ϕ(E>1.0 Mev) (n/cm^2)	Lead Factor	Vessel Fluence (n/cm^2)	Calculated Vessel Fluence (n/cm^2)
V	4.80×10^7	1.36×10^{11}	6.53×10^{18}	3.37	1.94×10^{18}	1.90×10^{18}
T	1.09×10^8	7.61×10^{10}	8.29×10^{18}	1.94	4.27×10^{18}	4.31×10^{18}
R	1.61×10^8	1.25×10^{11}	2.01×10^{19}	3.37	5.96×10^{18}	6.36×10^{18}

6.38×10^{18}, 8.35×10^{18}, and 2.14×10^{19} n/cm^2 for Capsules V, T, and R, respectively. Further, the graphical representation in figure 6-9 indicates the accuracy of the transport analysis for Point Beach Unit 2 and supports the use of the analytically determined fluence trend curve for predicting vessel toughness at times in the future. Projecting to end-of-life, a summary of peak fast neutron exposure of the Point Beach Unit 2 reactor as derived from both calculation and measurement may be made as follows.

	Fast Neutron Fluence (n/cm^2)		
	Surface	**1/4 T**	**3/4 T**
Capsule V	4.05×10^{19}	2.70×10^{19}	7.96×10^{18}
Capsule T	3.93×10^{19}	2.62×10^{19}	7.72×10^{18}
Capsule R	3.72×10^{19}	2.48×10^{19}	7.31×10^{18}
Average measurement	3.90×10^{19}	2.60×10^{19}	7.66×10^{18}
Calculation	3.96×10^{19}	2.64×10^{19}	7.78×10^{18}

These data are based on 32 full-power years of operation at 1518 MWt.

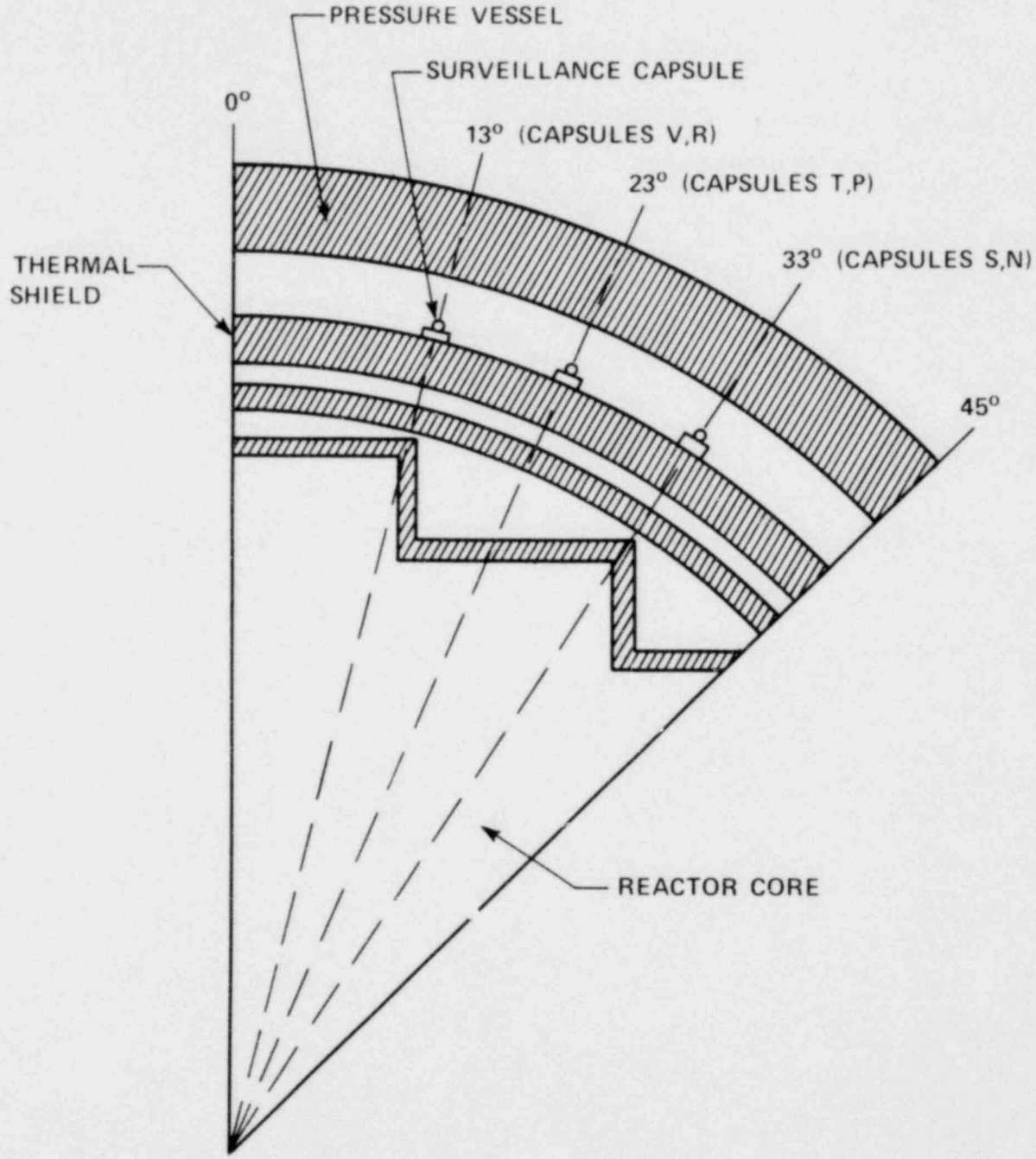

Figure 6-1. Point Beach Unit No. 2 Reactor Geometry

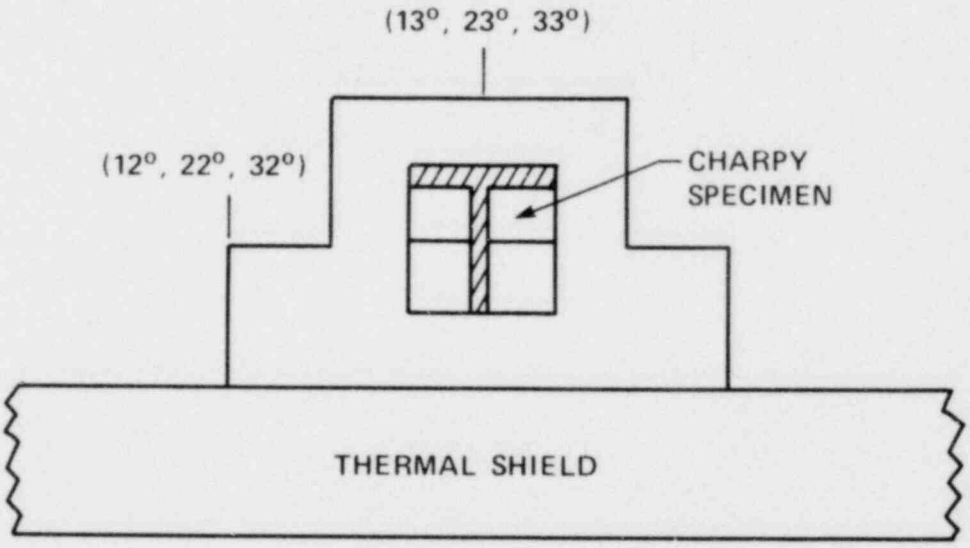

Figure 6-2. Plan View of a Reactor Vessel Surveillance Capsule

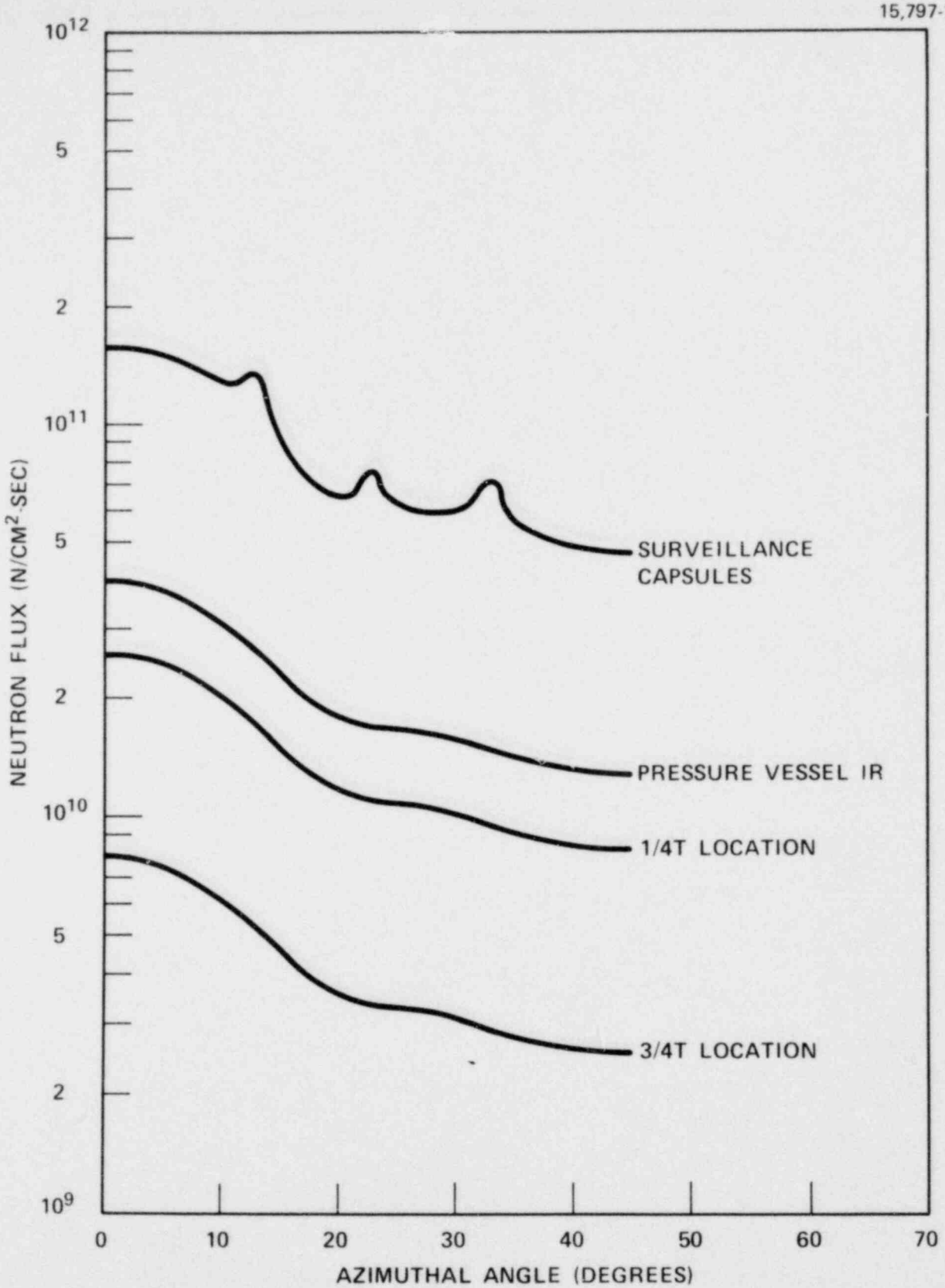

Figure 6-3. Calculated Azimuthal Distribution of Maximum Fast Neutron Flux (E > 1.0 Mev) Within the Pressure Vessel – Surveillance Capsule Geometry

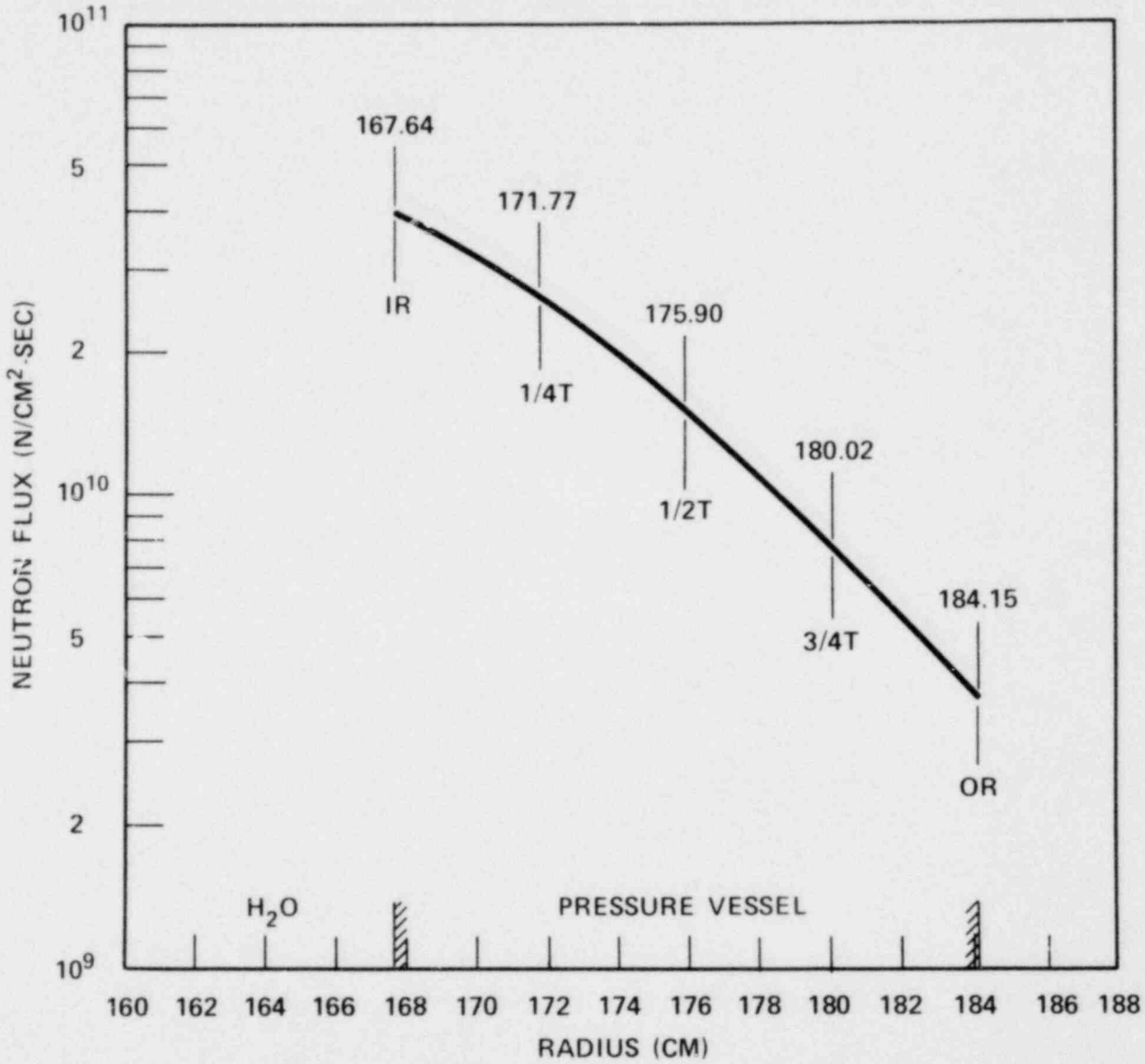

Figure 6-4. Calculated Radial Distribution of Maximum Fast Neutron Flux (E > 1.0 Mev) Within the Pressure Vessel

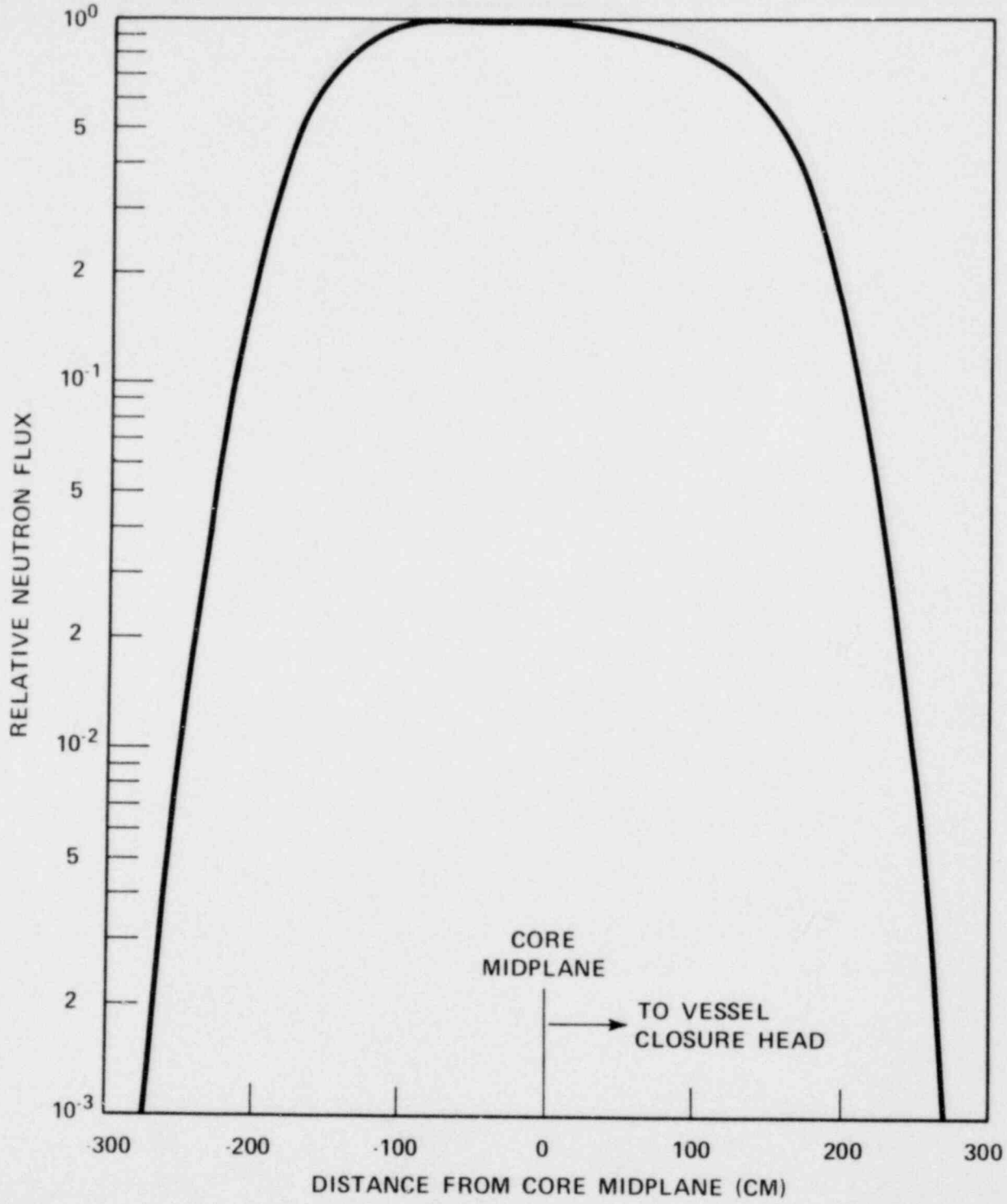

Figure 6-5. Relative Axial Variation of Fast Neutron Flux ($E > 1.0$ Mev) Within the Pressure Vessel

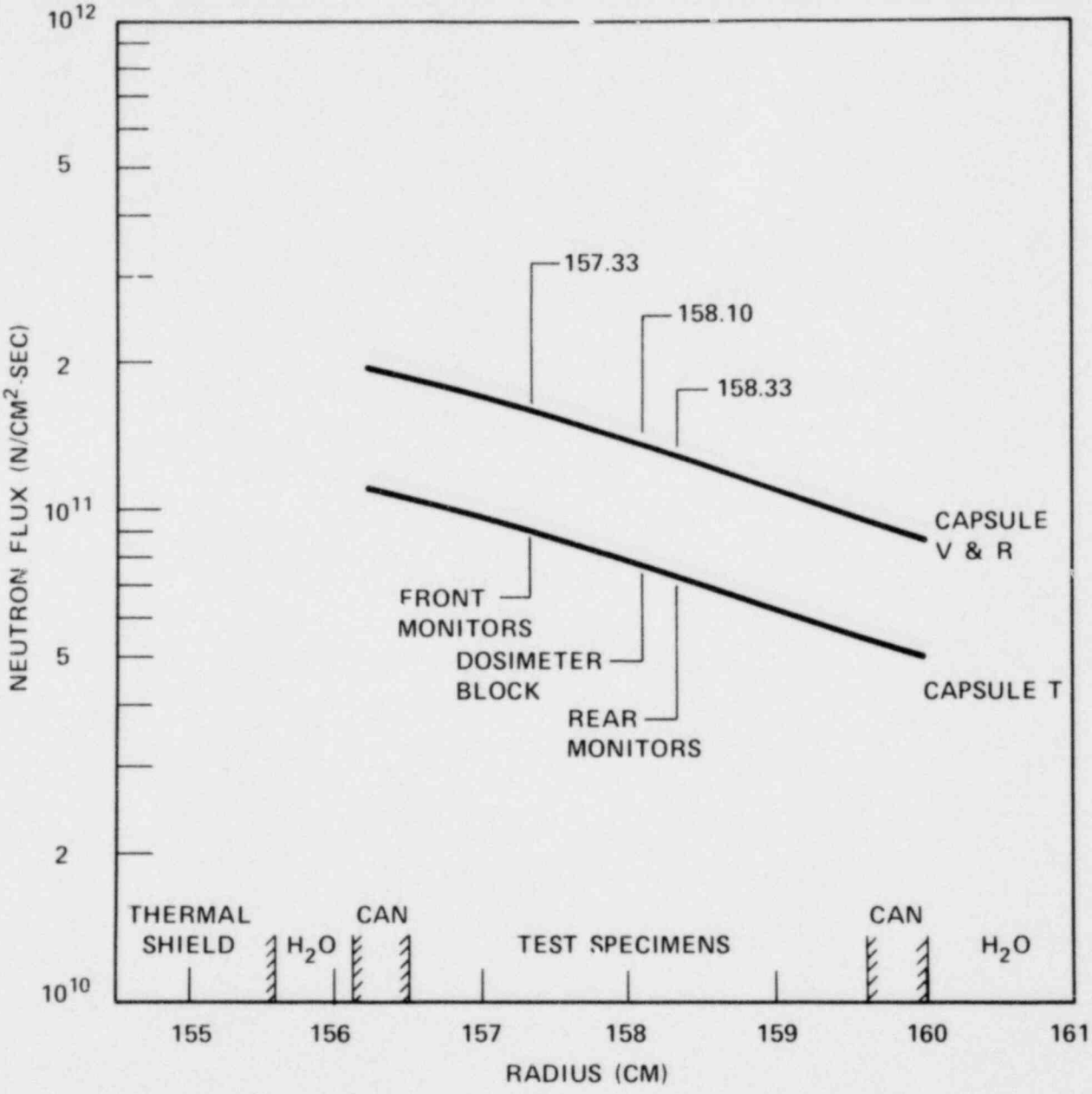

Figure 6-6. Calculated Radial Distribution of Maximum Fast Neutron Flux (E > 1.0 Mev) Within Surveillance Capsules V, R, and T

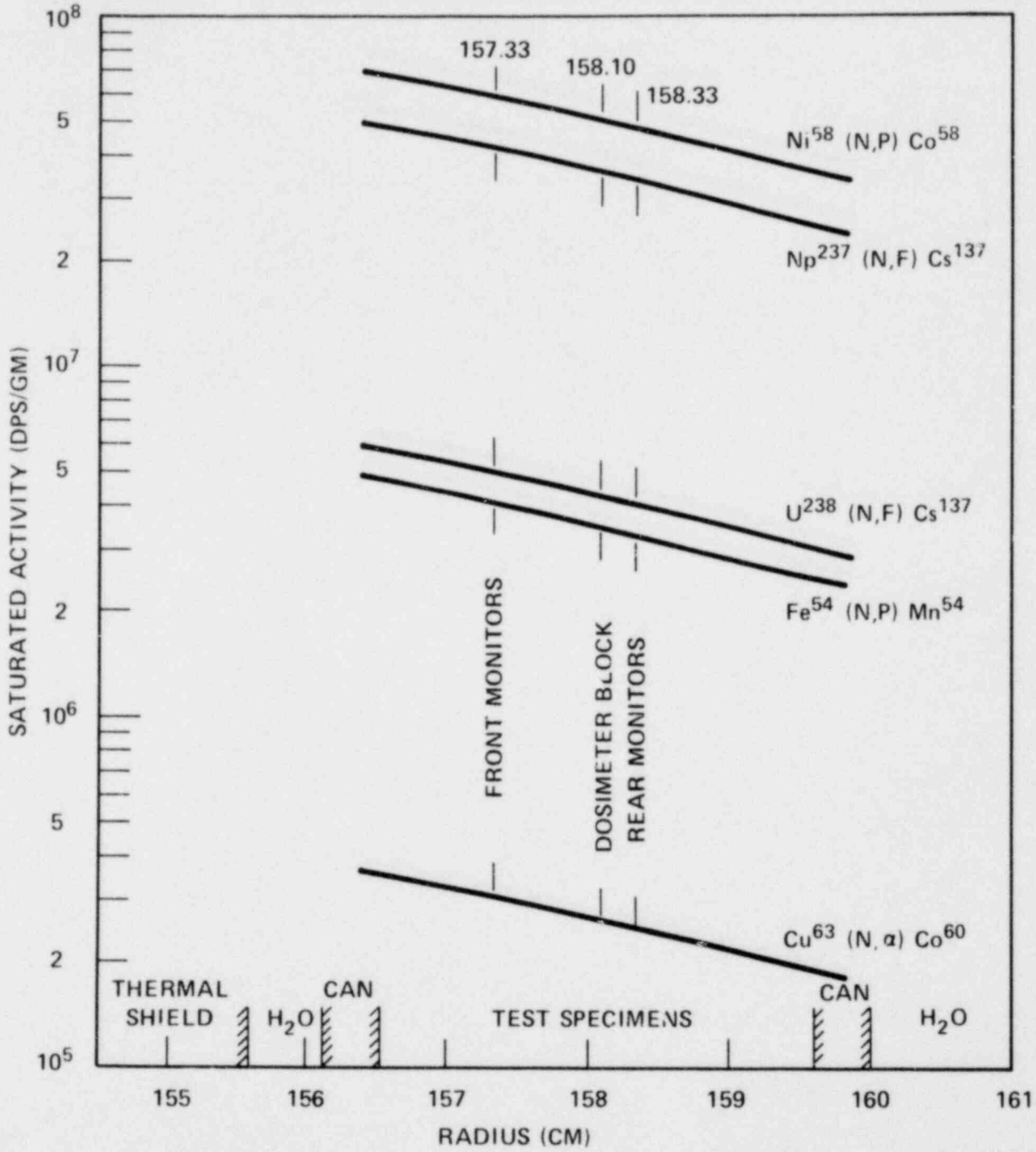

Figure 6-7. Calculated Variation of Fast Neutron Flux Monitor Saturated Activity Within Capsules V and R

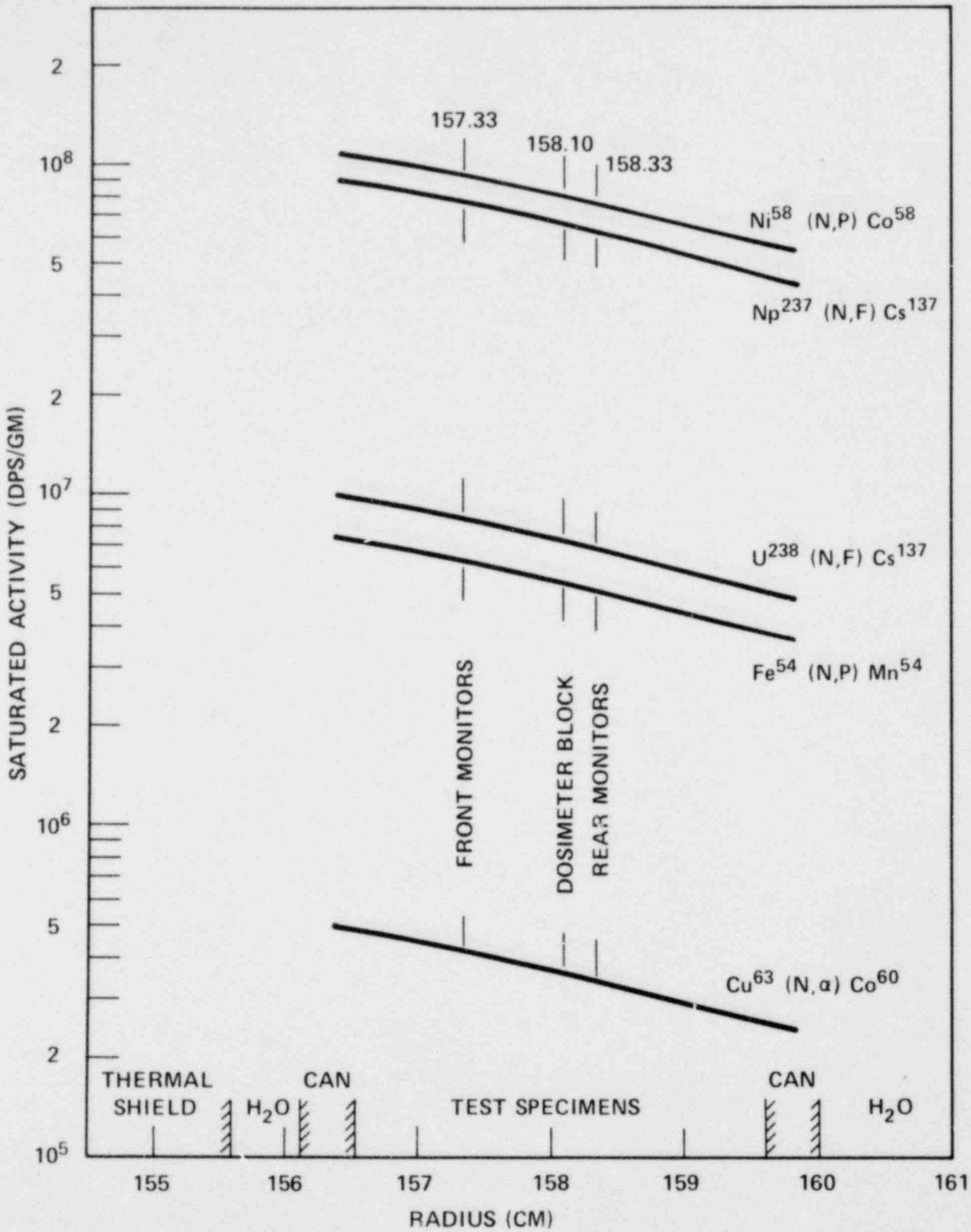

Figure 6-8. Calculated Variation of Fast Neutron Flux Monitor Saturated Activity Within Capsule T

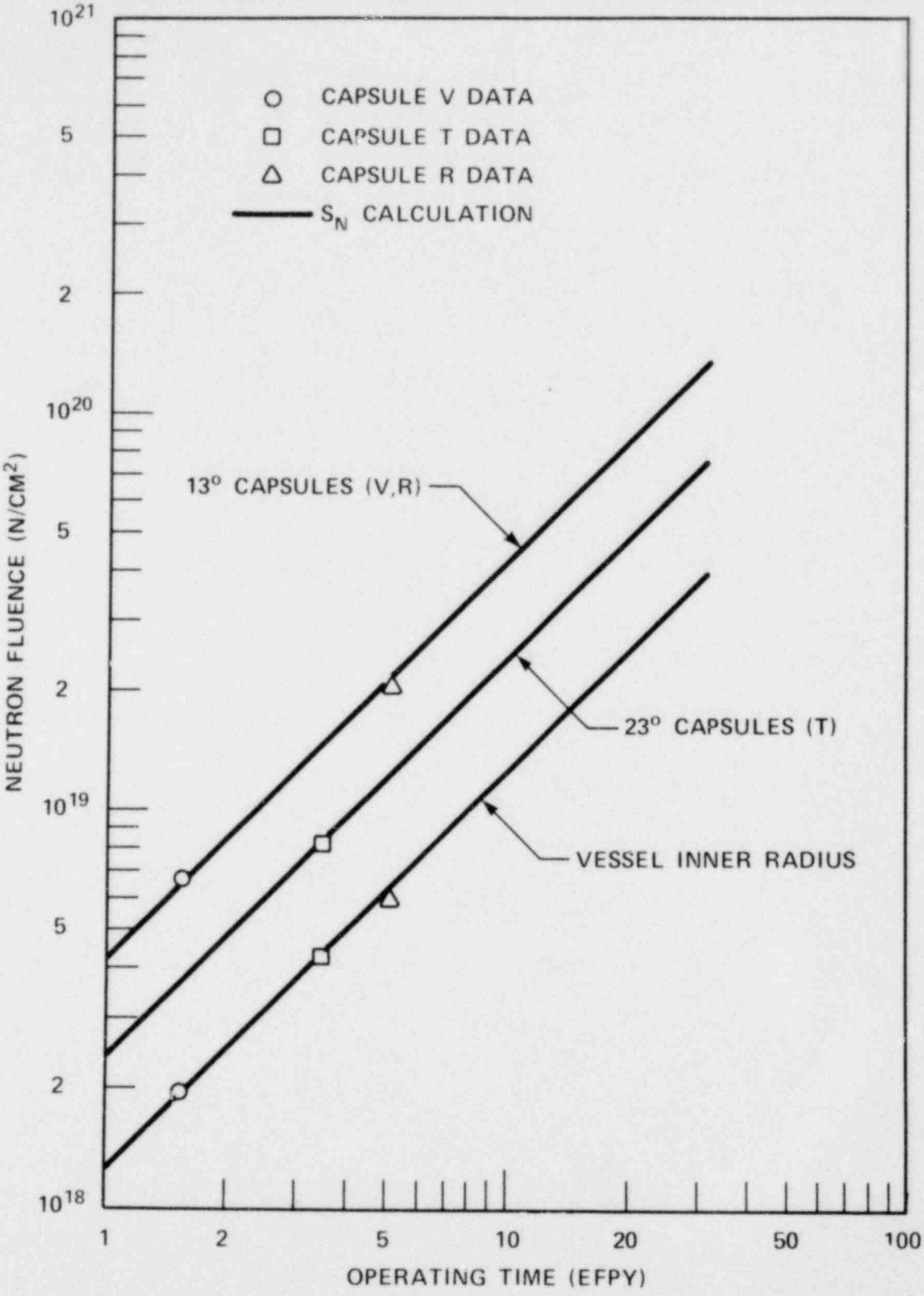

Figure 6-9. Comparison of Measured and Calculated Fast Neutron Fluence ($E > 1.0$ Mev) for Capsules V, T, and R

REFERENCES

1. Yanichko, S. E., and Zula, G. C., "Wisconsin Michigan Power Co., and the Wisconsin Electric Power Company Point Beach Unit No. 2 Reactor Vessel Radiation Surveillance Program," WCAP-7712, June, 1971.

2. ASTM Designation E185-66, "Surveillance Tests on Structural Materials in Nuclear Reactors," in ASTM Standards (1976), Part 31, Physical and Mechanical Testing of Metals – Metallography, Nondestructive Testing, Fatigue, Effect of Temperature, pp. 638-642, Am. Soc. for Testing and Materials, Philadelphia, Pa, 1967.

3. Perrin, J. S., Farmelo, D. R., Lowry, L. M., Wooton, R. D., and Denning, R. S., "Point Beach Unit No. 2 Pressure Vessel Surveillance Program: Evaluation of Capsule V," Battelle Research Report, June 10, 1975.

4. Davidson, J. A., Anderson, S. L., and Shogan, R. P., "Analysis of Capsule T from the Wisconsin Electric Power Company Point Beach Nuclear Plant Unit No. 2 Reactor Vessel Radiation Surveillance Program," WCAP-9331, August, 1978.

5. Soltesz, R. G., Disney, R. K., Jedruch, J. and Ziegler, S. L., "Nuclear Rocket Shielding Methods, Modification, Updating and Input Data Preparation. Vol. 5 – Two-Dimension Discrete Ordinates Transport Technique," WANL-PR(LL)034, Vol. 5, August 1970.

6. Collier, G., et al, "Second Version of the GAMBIT Code," WANL-TME-1969, November, 1969.

7. Soltesz, R. G., et al, "Nuclear Rocket Shielding Methods, Modification, Updating and Input Data Preparation – Volume 3, Cross-Section Generation and Data Processing Techniques," WANL-PR-(LL)-034, August, 1970.

8. Soltesz, R. G., et al, "Nuclear Rocket Shielding Methods, Modification, Updating and Input Data Preparation – Volume 4 – One-Dimensional Discrete Ordinates Transport Technique," WANL-PR-(LL)-034, August, 1970.

9. ASTM Designation E261-70, Standard Method for Measuring Neutron Flux by Radioactivation Techniques," in ASTM Standards (1975), Part 45, Nuclear Standards, pp. 745-755, Am. Society for Testing and Materials, Philadelphia, Pa., 1975.

10. ASTM Designation E262-70, "Standard Method for Measuring Thermal Nuetron Flux by Radioactivation Techniques," in ASTM Standards (1975), Part 45, Nuclear Standards, pp. 756-763, Am. Society for Testing and Materials, Philadelphia, Pa. 1975

REFERENCES (cont)

11. ASTM Designation E-263-70, "Standard Method for Measuring Fast-Neutron Flux by Radioactivation of Iron," in ASTM Standards (1975), Part 45, Nuclear Standards, pp. 764-769, Am. Society for Testing and Materials, Philadelphia, Pa., 1975.

12. ASTM Designation E481-73T, "Tentative Method of Measuring Neutron-Flux Density by Radioactivation of Cobalt and Silver," in ASTM Standards (1975), Part 45, Nuclear Standards, pp. 887-894, Am. Society for Testing and Materials, Philadelphia, Pa. 1975.

13. ASTM Designation E264-70, "Standard Method for Measuring Fast-Neutron Flux by Radioactivation of Nickel," in ASTM Standards (1975), Part 45, Nuclear Standards, pp. 770-774, Am. Society for Testing and Materials, Philadelphia, Pa., 1975.

14 Point Beach Nuclear Units 1 and 2 Semi-Annual Operating Reports, 1970 through 1979.